[AMERICAN JOURNAL OF SCIENCE, VOL. 296, MARCH, 1996, P. 244–295]

POLYMETAMORPHIC FLUID-ROCK INTERACTION OF THE TUDOR GABBRO AND ADJACENT MARBLE, ONTARIO

STEVEN R. DUNN* and JOHN W. VALLEY**

ABSTRACT. Polymetamorphism of the Tudor gabbro and adjacent marble, Grenville Province, southern Ontario, has caused a complex history in terms of temperature, time, and fluid conditions in a mid-crustal environment. Marble adjacent to the Tudor gabbro has undergone two metamorphic events; an early contact metamorphic aureole formed at ~1.24 Ga is overprinted by later regional metamorphism during the Grenville Orogeny (1.10 Ga). Seven mineral reaction isograds in marble are concentric to the gabbro contact. Phase equilibria and the chemical compositions of coexisting minerals were reset during lower amphibolite facies regional metamorphism at 485°C, 4 kb. Evidence of the earlier higher temperatures from near the gabbro contact is preserved in marble in the isotopic composition of coexisting calcite and graphite. Phase equilibria indicate a regular decrease in $X(CO_2)$ of regional metamorphic fluids approaching the gabbro from $X(CO_2) > 0.29$ in biotite-bearing marble over 2 km from the gabbro to $X(CO_2) = \sim 0.005$ adjacent to the contact.

The complexity of polymetamorphism is such that several P–T–time-X(fluids) paths may be hypothesized to arrive at the same final state. The data are best explained by the combined effects of a two-stage, polymetamorphic process. Volatilization reactions in the outer aureole proceeded in response to up-temperature fluid flow during contact metamorphism, and reactions in the inner aureole proceeded largely from thermal processes alone. Petrologic fluid fluxes for representative samples are from 60 to 530 moles/cm^2 for the contact metamorphism. Subsequent regional metamorphism involved the introduction of externally-derived, H_2O-rich fluid which locally infiltrated in a channelized manner resulting in fluid fluxes of 0 to ~10^5 moles/cm^2. This externally-derived fluid was focused along the gabbro-marble contacts resulting in infiltration-driven metamorphism of marble and hydration and carbonation of gabbro to metagabbro. Dehydration of lower crustal rocks at depth could provide more than sufficient quantities of water.

If the polymetamorphic nature of this aureole were not recognized, the isograd reactions would be considered products of regional metamorphism. This would erroneously suggest greater fluid fluxes for all samples and pervasive infiltration of all rocks for 3 km from the gabbro contact. The Tudor aureole serves as an example of how profoundly model-dependent fluid flow calculations are, especially in areas of multiple metamorphic events. Metamorphic fluid flow processes can only be understood if the full thermal history of a region is known.

INTRODUCTION

Fluids are important in the crust. They can transport matter and heat, control mineral equilibria and melting relations, and affect crustal

* Department of Geology and Geography, Mount Holyoke College, South Hadley, Massachusetts 01075.

** Department of Geology and Geophysics, University of Wisconsin, Madison, Wisconsin 53706.

properties such as rheology, seismic impedance, and electrical conductivity. Our understanding of fluid flow processes in the crust has advanced greatly in recent years from the evolution of hydrothermal systems in shallow crustal settings (for example, Taylor and Forester, 1979; Criss and Taylor, 1986; Manning and Bird, 1991) to fluid-rock interactions in the mid-crust (for example, Ferry, 1984, 1986, 1992; Baker and others, 1989) and to restricted fluid flow in deep crustal provinces (for example, Valley and others, 1990; Cartwright and Valley, 1991).

In spite of these advances, the nature of fluid flow in the mid-crust is not well understood and many uncertainties remain, in particular the quantities and directions of fluid flow. Theoretical models of fluid-controlled processes (for example, Walther and Orville, 1982; Etheridge, Wall, and Vernon, 1983; Bickle and McKenzie, 1987; Baumgartner and Rumble, 1988; Baumgartner and Ferry, 1991; Ferry and Dipple, 1991; Lasaga and Rye, 1993) must be evaluated in light of petrological evidence from metamorphic rocks. Petrologic studies of exposed portions of the paleo-mid-crust provide useful constraints on fluid compositions, quantities, sources, and migration mechanisms; however, these processes are complex, and the conditions that are deduced often depend upon the models assumed for fluid-mineral reaction.

In this study, we reconstruct the reaction history of polymetamorphosed marble in the contact aureole of the Tudor gabbro, southern Ontario. Mineral reaction isograds in marble adjacent to the Tudor gabbro are concentric to the gabbro. Both the contact metamorphosed marble and the gabbro itself have been regionally metamorphosed. The uniform temperature of regional metamorphism imprinted across the aureole requires a fluid composition anomaly (H_2O-rich) associated with the gabbro during the regional metamorphism. Because of the polymetamorphic setting, the formation of the reaction isograds can be modeled by more than one P–T–t–X(fluid) history. Vastly different interpretations of fluid flow processes result for the Tudor aureole depending on the reaction model adopted. Recognition of and proper accounting for polymetamorphism is essential for understanding fluid-rock interactions.

At Whetstone Lake, 15 km west of the Tudor area, Carmichael (1970) recognized intersecting mineral reaction isograds resulting from variations in pressure, temperature, and fluid composition. Such interplay between fluid composition, pressure, and temperature is important in determining local and regional patterns of fluid flow. Some of the mineral reaction isograds found around the Tudor gabbro also occur around other nearby intrusions (LeAnderson and Munoz, 1987) and have also been delineated on a regional scale by sampling metasediments distant from intrusive bodies (Sobol and Essene, 1973; Sobol, 1973). Isotherms and regional isograds are subparallel on a regional scale away from plutons, which implies that isograds are temperature controlled. However, localized regions of metamorphic "highs" and "lows" result

from smaller-scale fluid anomalies, such as at Tudor, and these have important implications for understanding crustal fluid processes.

Polymetamorphism presents complications for interpreting any fluid-dependent mineral reaction, because fluid conditions may differ from one metamorphic event to another. Reaction progress records the cumulative result of reactive fluid summed over the entire fluid-rock reaction history. Because reaction temperature greatly affects equilibrium fluid composition and, therefore, calculated fluid/rock ratios or fluxes, the accuracy of reaction progress methods depends on applying accurate reaction models. Fluid budgets are particularly difficult to reconstruct in polymetamorphic settings because the extent of reaction during each metamorphic event is generally unknown, and reaction temperatures, pressures, and fluid compositions during early events become obscured or reset by later events.

In many ways, our understanding of P–T–t histories of metamorphic rocks has advanced more quickly than our understanding of fluid-rock interactions in the mid-crust. This might be expected given that determining the composition of a metamorphic fluid, a common starting point, requires P–T information. Many studies of metamorphic fluids ignore the temporal aspect of metamorphism by focusing mainly on peak P–T conditions. As our knowledge of P–T–t paths for specific terranes improves, models that incorporate P–T–t–X(fluid) will have to be developed that are consistent with this broader perspective.

GEOLOGICAL SETTING

The study area is within the Central Metasedimentary Belt of the Grenville Province which contains the most extensive sequence of supracrustal rocks found in the southern Grenville. These rocks consist of metasedimentary rocks with a high proportion of marble and calcareous rocks and also include metamorphosed volcanic rocks including pillow lavas, hydrothermally altered sea-floor basalts, and pyroclastic rocks. Numerous mafic plutons, including the Tudor gabbro, have been emplaced throughout the terrane, and granitic to syenitic intrusive rocks are abundant as well (fig. 1). In contrast to most of the Grenville Province which contains upper amphibolite and granulite facies rocks, the Central Metasedimentary Belt is of lower grade, greenschist to middle amphibolite facies (Carmichael, Moore, and Skippen, 1978; Anovitz and Essene, 1989). In the study area, regional metamorphism was of lower amphibolite facies.

Geochronology indicates that at least one episode of regional metamorphism postdates the intrusion of mafic plutons in the Central Metasedimentary Belt by 100 Ma. The metavolcanic country-rocks intruded by the Tudor gabbro have a whole-rock Rb-Sr isochron age of 1250 ± 90 Ma (Bell and Blenkinsop, 1980) and a U-Pb zircon age of 1286 ± 15 Ma (Silver and Lumbers, 1966; Easton, 1986). Titanite from a calc-silicate gneiss near the Tudor contact yields a U-Pb age of 1240 ± 2 Ma (Mezger and others, 1993). Similar ages are obtained for other mafic

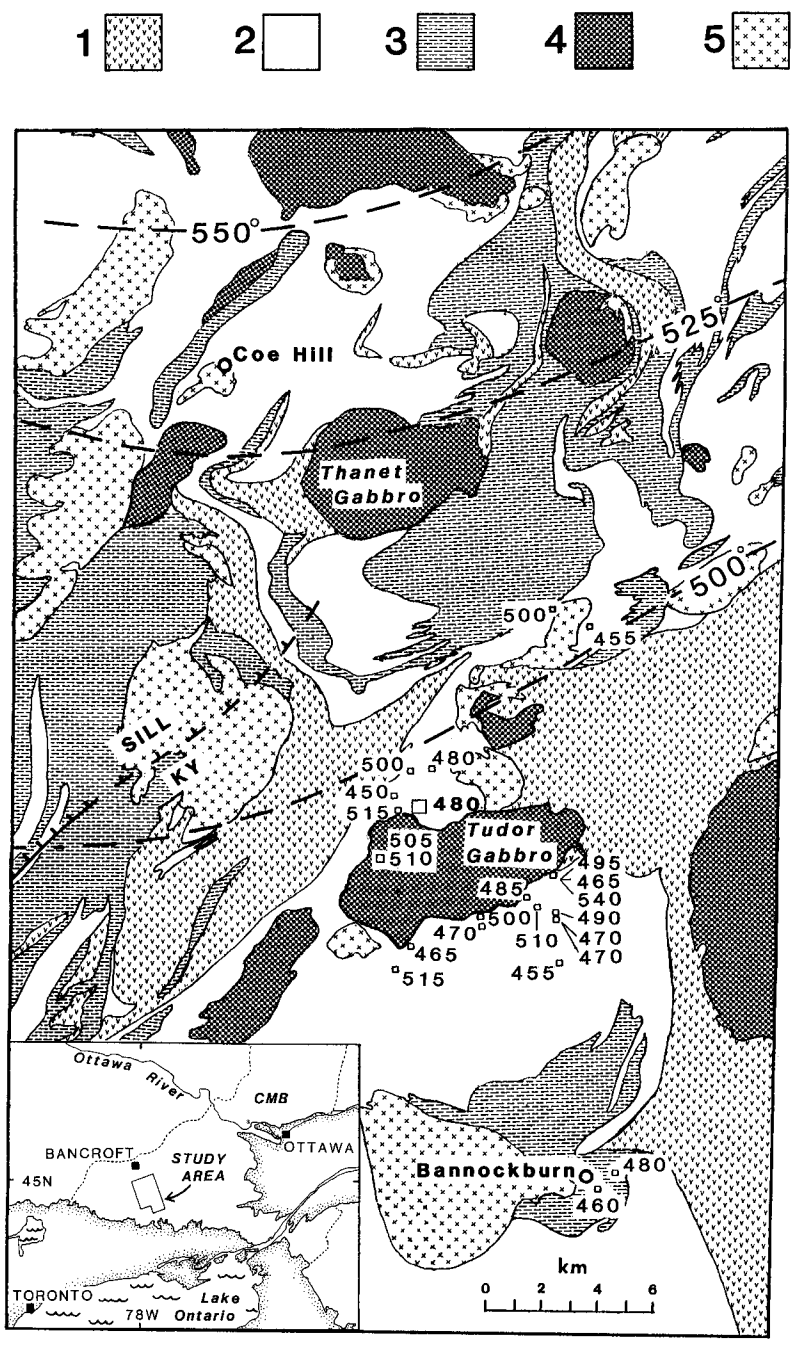

Fig. 1. Generalized geologic map of the Tudor area, Ontario, simplified from Shaw (1962), Hewitt (1962, 1968), Laakso (1968), and Lumbers (1969). The inset shows extent of exposed Precambrian rocks (unpatterned, CMB = Central Metasedimentary Belt) and Phanerozoic rocks (stippled edges). Legend: 1 = metavolcanic rocks, 2 = marble, 3 = siliceous metasedimentary rocks, 4 = gabbroic intrusive rocks, 5 = granitic and syenitic intrusive rocks. Metamorphic temperatures (°C) shown are determined from calcite-dolomite solvus thermometry (table 2). The square labelled 480 near the northern contact of the Tudor gabbro represents the average temperature for eleven samples within a 600 × 600 m area. The regional isotherms are also from calcite-dolomite thermometry (Sobol, 1973; Sobol and Essene, 1973), and the kyanite-sillimanite isograd is mapped by Carmichael (1970).

plutons in the region. The Cordova gabbro, 25 km to the south, yields a U-Pb age for zircon of 1242 ± 3 Ma (Davis and Bartlett, 1988). K-Ar and Ar-Ar dating of whole-rocks and hornblende separates from the Tudor gabbro and the Thanet gabbro (15 km north of the Tudor) yield ages of 1200 Ma and younger which are likely to reflect cooling ages and/or partial post-crystallization resetting and might also reflect some recrystallization during regional metamorphism (Hayatsu and Palmer, 1975; Berger and York, 1981; Baksi, 1982; Cosca, Sutter, and Essene, 1991). Regional metamorphism in the area occurred between 1102 and 1088 Ma based on ages of deformed and metamorphosed versus undeformed and unmetamorphosed intrusive rocks (Davis and Bartlett, 1988; Corriveau and others, 1990) and also from ages of accessory titanite within marble and calc-silicate gneiss (Mezger and others, 1993).

The Tudor Gabbro

The ovoid Tudor gabbro (~9 × 4 km) is emplaced into marble and metavolcanic country-rocks (fig. 1). The pluton is dominantly gabbro with less abundant pyroxenite and anorthositic gabbro, all of which display variable degrees of metamorphic recrystallization. Igneous mineral assemblages in gabbro consist of clinopyroxene (titanaugite) + labradorite (~An50-An60) + magnetite ± hornblende ± orthopyroxene ± olivine. Coarse- to medium-grained subhedral granular textures predominate, but subophitic and anhedral granular textures are also common. Metamorphic recrystallization proceeded initially along grain boundaries by conversion of clinopyroxene to amphibole + ilmenite ± calcite ± titanite and conversion of labradorite to epidote + albite ± oligoclase ± calcite. Less commonly, minor amounts of biotite, chlorite, or scapolite coexist with the metamorphic assemblage. Where metamorphic recrystallization is complete, samples commonly retain the textural appearance of their igneous precursor with fine-grained amphibole pseudomorphs after clinopyroxene and very finely intergrown albite + epidote after labradorite. The metamorphic recrystallization is readily recognizable in hand sample as the dark, glassy igneous plagioclase becomes beige to milky yellow or yellowish-green. Metasomatized gabbro occurs locally at some marble contacts consisting of sugary-textured endoskarns in variegated shades of green due to varying proportions of epidote, amphibole, and albite.

Country-Rocks

Country-rocks in the area include marble, siliceous metasedimentary rocks, and metavolcanic rocks (fig. 1). Marble in Tudor and Lake Townships is typically fine-grained, dark gray, and layered on the scale of centimeters. It consists predominately of calcite, and most samples contain quartz, albite, and biotite. Chlorite and dolomite are also common, and accessories include graphite, rutile, pyrrhotite, and, rarely, muscovite. Siliceous metasedimentary rocks are typically fine-grained, weakly foliated, light to dark gray or brownish in color, layered on the scale of

centimeters to decimeters, and sometimes show sedimentary grading. These rocks contain abundant quartz and albite, variable amounts of biotite, calcite, chlorite, and muscovite, and minor pyrrhotite. Metavolcanic rocks to the north and east of the Tudor gabbro are mainly basaltic lithologies consisting of pillowed flows and fragmental units with subordinate intermediate and felsic members. Typical mafic metavolcanic rocks contain albite, epidote, chlorite, and amphibole, and accessories include quartz, calcite, titanite, biotite, ilmenite, pyrrhotite, and pyrite.

This study focuses on the large expanse of marble south of the Tudor gabbro shown in figure 1. Marble and calcite-rich lithologies are dominant in this area; however the calcite contents of individual layers range from 99 to < 1 modal percent. Several carbonate-poor siliceous metasedimentary units occur within the marble near the Tudor gabbro, but even these units contain some carbonate-rich layers (fig. 2; Lumbers, 1969). The distinction between marble and siliceous metasedimentary rocks is normally based on the percentage of carbonate present; however there is complete gradation between these rock types, and they are interbedded on various scales. Thus in this study the term "marble" is used loosely to refer to all the country-rock dominated by carbonate.

Marble has been modified near contacts with the Tudor gabbro and other plutons in the region. Away from igneous contacts, marble is fine-grained and medium to dark gray in color due to finely disseminated graphite and/or pyrrhotite. Approaching igneous contacts, marble coarsens and becomes lighter in color primarily as a result of the coalescence of very finely disseminated graphite (Dunn and Valley, 1992). A sequence of mineral reaction isograds developed in the marble are concentric to the Tudor gabbro. These reactions are described more fully in the following section.

ISOGRADS IN MARBLE

Seven reaction isograds based on isobarically univariant reactions are recognized in marble south of the Tudor gabbro. The positions of these and other isograds both north and south of the Tudor gabbro were first determined by Allen (1976). In this study, petrographic examination of over 160 marble samples combined with staining methods and electron microprobe analysis has allowed us to refine the position of these isograds in the marble south of the Tudor gabbro. Complete mineral assemblage and locality data for samples utilized in this study are given in Dunn (1989).

Mineral reactions pertinent to equilibria in impure marbles are listed in table 1. The regional metamorphic grade is above reaction 1; biotite + calcite assemblages are common in the area, and K-feldspar + dolomite assemblages are absent. Isograds at Tudor correspond to reactions 2 through 8, which represent, in order of increasing grade, the first appearance of titanite, amphibole, amphibole + clinozoisite, amphibole + K-feldspar, clinopyroxene, clinopyroxene + biotite, and garnet, in rocks of appropriate composition (fig. 3, A-F). Our observations and

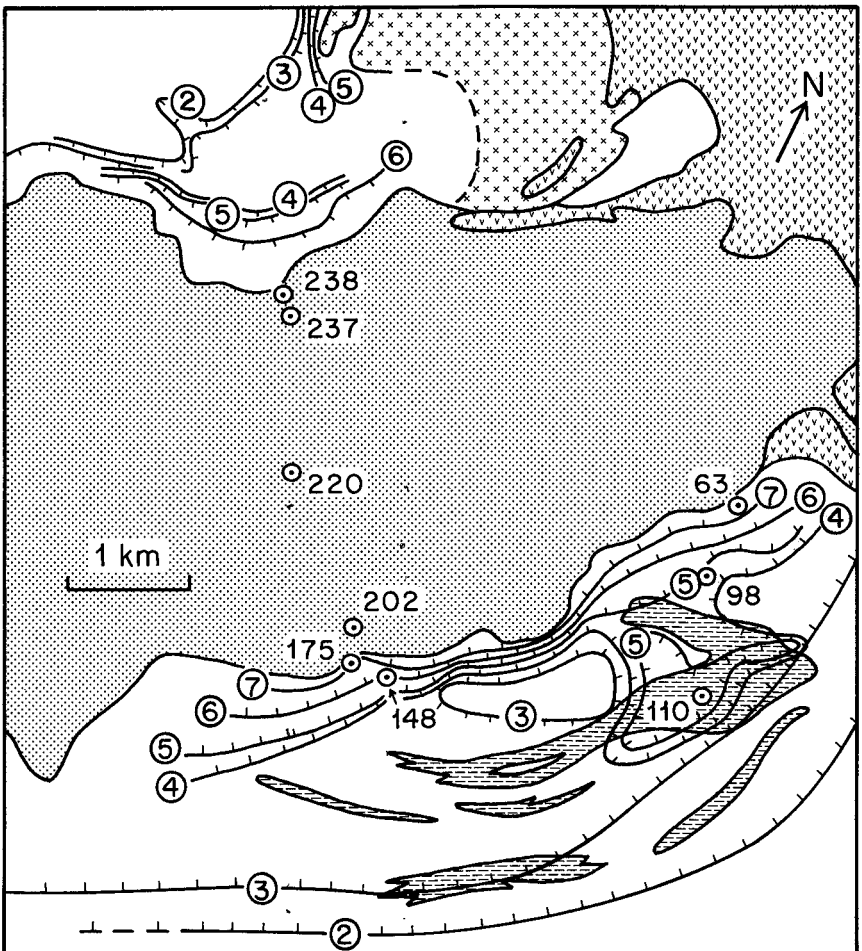

Fig. 2. Location of all isograds about the Tudor gabbro. Isograds south of the Tudor gabbro (fig. 3A-F) and those to its north (Allen, 1976) are concentric about the pluton indicating that $X(H_2O)$ in the regional metamorphic fluid increased toward the gabbro. The locations of samples described in the text are shown (numbers). Lithologies are patterned as in figure 1 except the gabbro is more lightly stippled. The siliceous metasedimentary rocks immediately south of the gabbro were omitted from figure 1 for clarity. The coincidence of a localized metamorphic "high" (around sample 110), and the region of abundant siliceous metasediments suggests locally higher $X(H_2O)$ associated with these carbonate-poor rocks.

placement of isograds are consistent with Allen (1976), although he did not map isograd 7 (clinopyroxene + biotite). The isograds are concentric about the gabbro along both the southern and northern margins (fig. 2). The position of the garnet isograd (8), which is omitted from figure 2 for clarity, is poorly constrained as only three garnet-bearing samples have

TABLE 1

Reactions pertinent to metamorphism of Tudor marbles

(1) $Kfs + 3Dol + H_2O = Phl + 3Cal + 3CO_2$
(2) $Rt + Cal + Qtz = Ttn + CO_2$
(3) $5Dol + 8Qtz + H_2O = Tr + 3Cal + 7CO_2$
(4) $3Chl + 10Cal + 21Qtz = 3Tr + 2Czo + 10CO_2 + 8H_2O$
(5) $5Phl + 6Cal + 24Qtz = 3Tr + 5Kfs + 6CO_2 + 2H_2O$
(6) $Tr + 3Cal + 2Qtz = 5Di + 3CO_2 + H_2O$
(7) $3Tr + 6Cal + Kfs = 12Di + Phl + 6CO_2 + 2H_2O$
(8) $2Czo + 5Cal + 3Qtz = 3Grs + 5CO_2 + H_2O$
(9) $3An + Cal + H_2O = 2Czo + CO_2$
(10) $Tr + 3Cal = 4Di + Dol + CO_2 + H_2O$
(11) $Di + 3Dol = 2Fo + 4Cal + 2CO_2$
(12) $Tr + 11Dol = 8Fo + 13Cal + 9CO_2 + H_2O$
(13) $3Tr + 5Cal = 11Di + 2Fo + 5CO_2 + 3H_2O$
(14) $Cal + Qtz = Wo + CO_2$
(15) $An + 2Cal + Qtz = Grs + 2CO_2$
(16) $4Czo + Qtz = 5An + Grs + 2H_2O$
(17) $2Dol + Phl + 8Qtz = Tr + Kfs + 4CO_2$
(18) $Dol + 2Qtz = Di + 2CO_2$
(19) $Tr + 2Dol + Kfs = 4Di + Phl + 4CO_2$

Abbreviations and formulas: Am = amphibole; An = anorthite, $CaAl_2Si_2O_8$; Bi = biotite; Cal = calcite, $CaCO_3$; Chl = chlorite, $Mg_5Al_2Si_3O_{10}(OH)_8$; Czo = clinozoisite, $Ca_2Al_3Si_3O_{12}(OH)$; Cpx = clinopyroxene; Di = diopside, $CaMgSi_2O_6$; Dol = dolomite, $CaMg(CO_3)_2$; Fo = forsterite, Mg_2SiO_4; Gr = graphite; Grs = grossular, $Ca_3Al_2Si_3O_{12}$; Kfs = potassium feldspar, $KAlSi_3O_8$; Ms = muscovite; Ol = olivine; Phl = phlogopite, $KMg_3AlSi_3O_{10}(OH)_2$; Pl = plagioclase; Po = pyrrhotite; Py = pyrite; Qtz = quartz, SiO_2; Rt = rutile, TiO_2; Tlc = talc; Tr = tremolite, $Ca_2Mg_5Si_8O_{22}(OH)_2$; Ttn = titanite, $CaTiSiO_5$; Tur = tourmaline; Wo = wollastonite, $CaSiO_3$.

been found along the southern margin of the gabbro, but it nearly coincides with isograd 7.

No isograd is mappable for reaction 9, the clinozoisite reaction, due to the sporadic occurrence of reactant and product assemblages (fig. 3G). More than 2 km from the gabbro, only reactant assemblages occur (plagioclase + calcite). Within two km, reactant-only and product-only assemblages are found, but assemblages with both reactants and products dominate (fig. 3G). If an isograd were to be placed at the first appearance of clinozoisite, it would essentially coincide with the amphibole + clinozoisite isograd (isograd 4).

Allen (1976) described talc-bearing assemblages essentially coincident with isograd 3 around the northern margin of the Tudor gabbro. However, in the southern Tudor aureole, talc-bearing assemblages are rare, and textures often indicate a secondary or retrograde origin. No reaction isograds involving talc could be delineated in this study.

Forsterite-bearing marble occurs within a xenolith in the gabbro near its western margin (fig. 1, next to temperatures 505 and 510). This coarse, white to light gray banded marble and calc-silicate contains calcite + forsterite and thus corresponds to the products of reactions 11 and 12. Dolomite, graphite, pyrrhotite, and chlorite are also common in the xenolith. No forsterite has been found in marble elsewhere, and, thus, no forsterite isograd is defined.

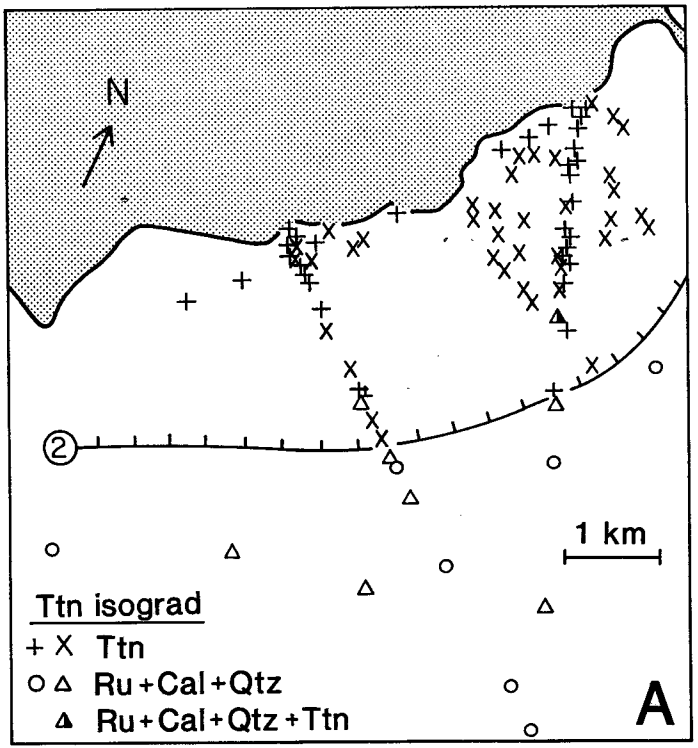
N
2
1 km
Ttn isograd
+ X Ttn
○ △ Ru+Cal+Qtz
▲ Ru+Cal+Qtz+Ttn
A

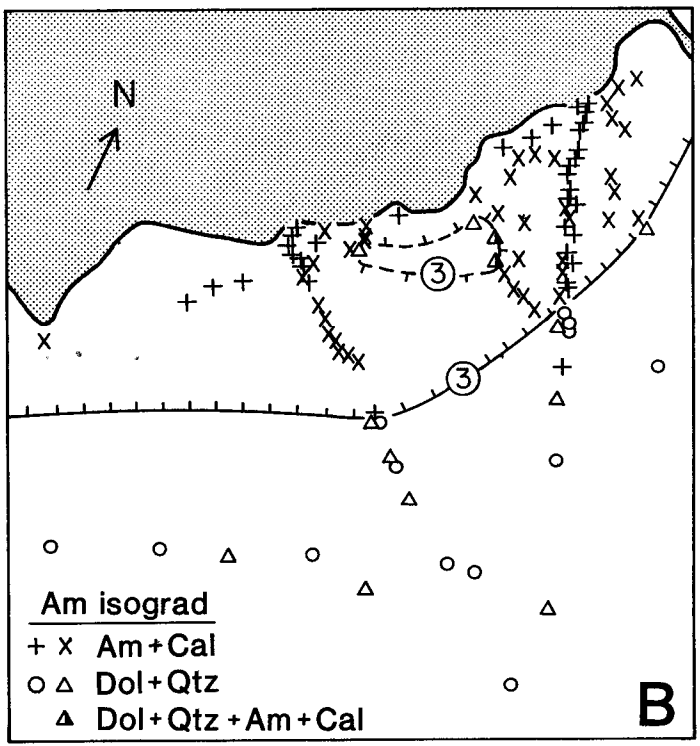
N
3
3
Am isograd
+ X Am+Cal
○ △ Dol+Qtz
▲ Dol+Qtz+Am+Cal
B

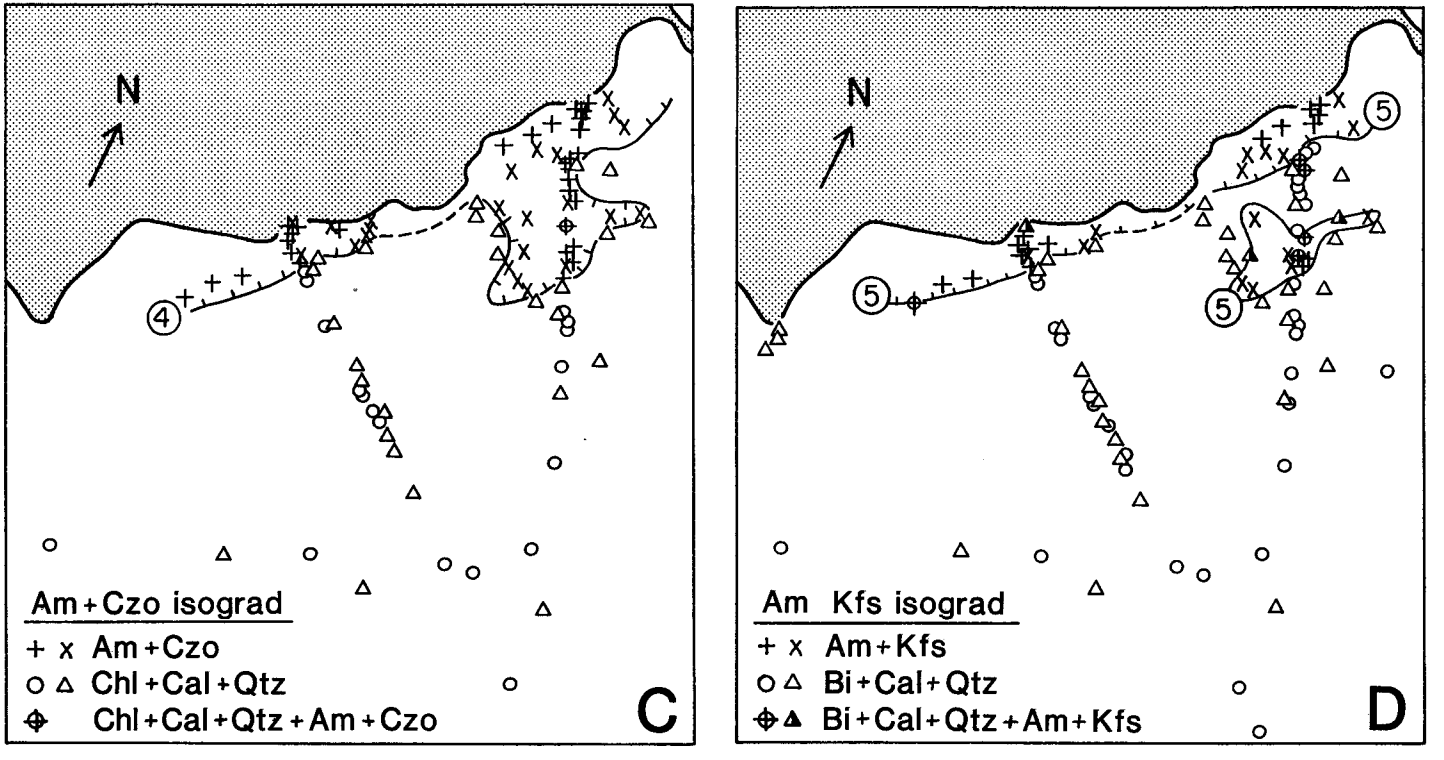

Fig. 3. Location of pertinent mineral assemblages and reaction isograds in marble south of the Tudor gabbro (stippled). Reactant assemblages are shown as open circles (this study) and triangles (Allen, 1976), product assemblages are shown as +'s (this study) and x's (Allen, 1976), univariant assemblages (reactant and product) are shown as encircled +'s (this study) and half-filled triangles (Allen, 1976). A to F correspond to reactions 2 to 7 in table 1. The open arrow in F shows the location of sample #175 which contains the univariant assemblage of reaction 8, thus, isograd 8 (left off for clarity) is essentially coincident with isograd 7. G corresponds to reaction 9 for which no isograd can be delineated (see text).

Fig. 3 (continued)

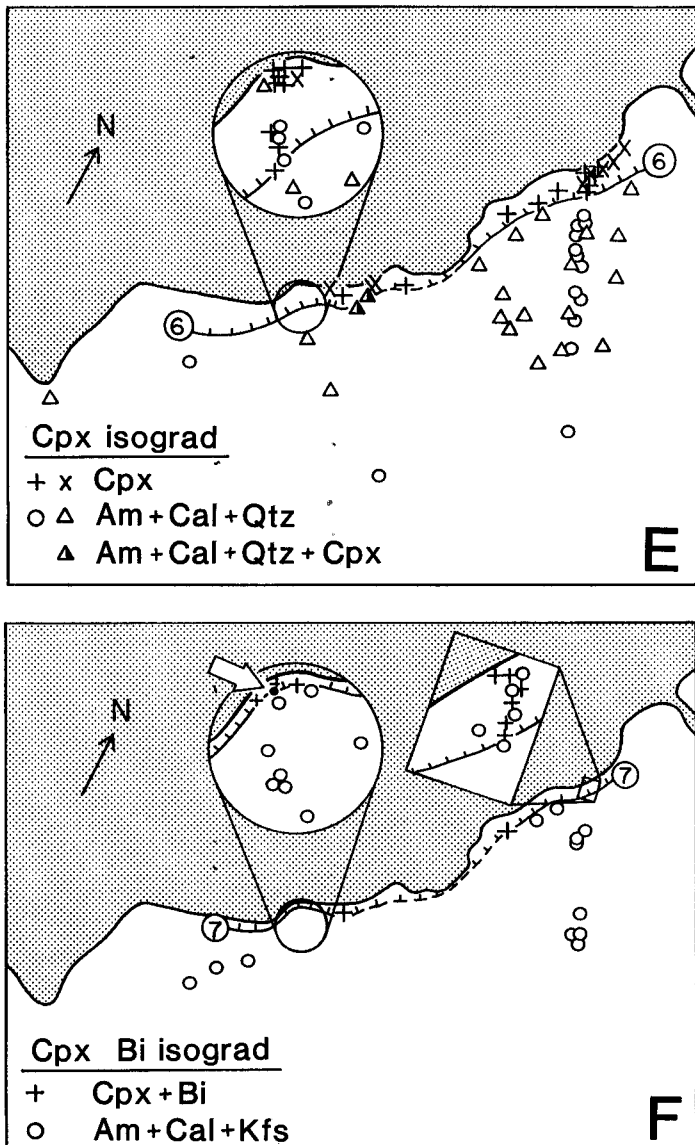

METAMORPHIC CONDITIONS

Regional Metamorphism

Temperatures of regional metamorphism have been determined by calcite-dolomite solvus thermometry in four independent studies, two of

Fig. 3 (continued)

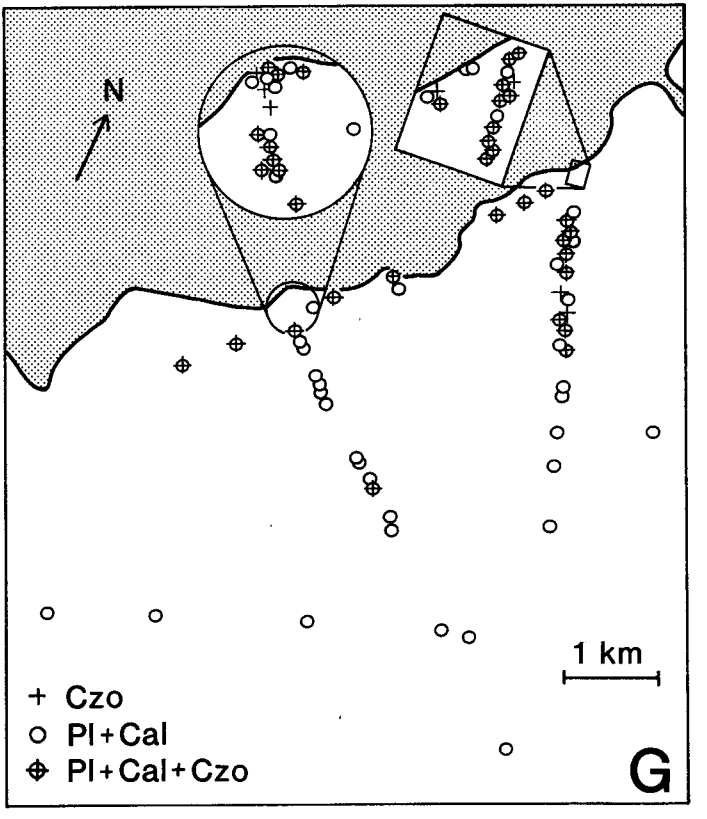

the immediate area around the Tudor gabbro (Allen, 1976; Dunn, 1989; Dunn and Valley, 1992) and two of regional scale (Sobol and Essene, 1973; Rathmell, Essene, and van der Pluijm, in submission); all are in excellent agreement for the Tudor area. Calcite compositions from Allen (1976) and from this study were used to determine solvus temperatures, accounting for the Fe content of calcite (table 2). Nine samples from this study, ranging from 7 km north of the gabbro to 11 km south of the gabbro (fig. 1), yield an average temperature of 470°C ± 13° (1σ). Two additional samples from the marble xenolith described earlier yield temperatures of 505° and 510°C. Twenty-two samples from the same area reported by Allen (1976) yield an average temperature of 490°C ± 24° (1σ). The combined data sets (Allen, 1976, and this study) yield an average of 485°C ± 20° (1σ) for 34 samples without any thermal aureole associated with the gabbro and independent of sample mineralogy (fig. 1; table 2). These temperatures reflect post-intrusion, regional metamor-

TABLE 2

Calcite compositions, temperatures estimated from the calcite-dolomite solvus, and primary mineral assemblages for marble around the Tudor gabbro

Sample	X(Ca)	X(Mg)	X(Fe)	X(Mn)	m to ctc*	°C**	Assemblage***
82	0.954	0.041	0.005	0.000	127 S	495	Cal, Dol, Bi, Am, Chl, Tlc, Po
83	0.962	0.036	0.002	0.000	128 S	465	Cal, Dol, Bi, Chl, Tlc, Gr
144	0.955	0.034	0.011	0.000	800 S	470	Cal, Dol, Am, Ttn, Pl, Chl
117	0.955	0.035	0.010	0.000	1,800 S	470	Cal, Dol, Qtz, Bi, Pl, Gr
118	0.953	0.034	0.012	0.001	1,800 S	470	Cal, Dol, Qtz, Bi, Pl, Chl, Po
125	0.958	0.032	0.010	0.000	3,000 S	455	Cal, Dol, Qtz, Bi, Pl, Chl, Po, Rt
259	0.949	0.030	0.018	0.003	11,000 S	460	Cal, Dol, Qtz, Bi, Pl, Chl, Po
260	0.949	0.036	0.013	0.002	10,500 S	480	Cal, Dol, Qtz, Bi, Pl, Kfs, Ms
258	0.963	0.034	0.003	0.000	7,000 N	455	Cal, Dol, Py, Po
225	0.953	0.044	0.002	0.001	~5 X	505	Cal, Dol, Ol, Po, Ttn, Chl, Gr
226	0.954	0.045	0.001	0.000	~5 X	510	Cal, Dol, Ol, Po, Gr
JA†-2	0.959	0.040	0.001	0.000	565 N	485	Cal, Dol, Qtz, Bi, Pl, Kfs, Ms, Rt, Py, Gr
JA-4	0.959	0.035	0.006	0.000	330 N	465	Cal, Dol, Qtz, Bi, Kfs, Rt, Py, Gr
JA-6	0.958	0.031	0.008	0.003	435 N	450	Cal, Dol, Qtz, Bi, Pl, Kfs, Rt, Po, Gr
JA-8	0.948	0.035	0.016	0.001	1,610 N	480	Cal, Dol, Qtz, Bi, Pl, Ms, Chl, Rt, Py, Po, Gr
JA-9	0.936	0.037	0.027	0.000	1,300 N	500	Cal, Dol, Qtz, Bi, Pl, Ms, Chl, Rt, Po
JA-10	0.957	0.033	0.010	0.000	1,090 N	460	Cal, Dol, Qtz, Bi, Pl, Ms, Chl, Rt, Po, Gr
JA-11	0.952	0.034	0.011	0.003	495 N	470	Cal, Dol, Qtz, Bi, Pl, Ms, Chl, Rt, Po, Cpy, Gr
JA-12	0.954	0.035	0.009	0.002	700 N	470	Cal, Dol, Qtz, Bi, Am, Ttn, Pl, Chl, Po, Gr
JA-13	0.951	0.037	0.010	0.002	450 N	480	Cal, Dol, Qtz, Bi, Am, Ttn, Pl, Chl, Po, Gr
JA-14	0.960	0.033	0.007	0.000	375 N	460	Cal, Dol, Qtz, Bi, Am, Ttn, Chl, Tlc, Gr
JA-15	0.956	0.036	0.007	0.001	240 N	475	Cal, Dol, Qtz, Bi, Am, Ttn, Chl, Tur, Po, Gr
JA-16††	0.930	0.036	0.030	0.004	7,500 N	500	Cal, Dol, Qtz, Bi, Am, Pl, Chl, Ilm
JA-17	0.954	0.037	0.007	0.002	270 N	480	Cal, Dol, Qtz, Am, Ttn, Tlc, Po, Gr
JA-18	0.941	0.048	0.011	0.000	400 N	530	Cal, Dol, Qtz, Bi, Am, Ttn, Pl, Chl, Tur, Gr
JA-24	0.950	0.042	0.005	0.003	430 N	500	Cal, Dol, Qtz, Pl, Ms, Rt, Tur, Py, Po
JA-25	0.942	0.053	0.002	0.003	25 S	540	Cal, Dol, Cpx, Ol, Po, Spinel
JA-26	0.953	0.039	0.006	0.002	150 S	485	Cal, Dol, Am, Chl, Tc, Gr
JA-27	0.945	0.044	0.008	0.003	600 S	510	Cal, Dol, Qtz, Bi, Am, Ttn, Chl, Gr
JA-28	0.949	0.038	0.013	0.000	1,500 S	490	Cal, Dol, Qtz, Bi, Ttn, Pl, Chl, Rt, Gr
JA-29	0.950	0.042	0.006	0.002	20 S	500	Cal, Dol, Am, Chl
JA-30	0.962	0.035	0.003	0.000	30 S	465	Cal, Dol, Bi, Ol, Tur, Po
JA-31	0.947	0.045	0.008	0.000	1,100 S	515	Cal, Dol, Qtz, Bi, Ttn, Chl, Gr
JA-32	0.951	0.046	0.002	0.001	<20 N	515	Cal, Dol, Am

* Meters to nearest contact with Tudor gabbro: S, southern contact; N, northern contact; X, xenolith.
** Calculated using the formulation of Anovitz and Essene (1987), rounded to nearest 5.
*** Abbreviations as in table 1.
† Samples JA- and compositions are from Allen (1976).
†† This sample is ~100 m from the granitic Beaver Creek intrusive complex.

phic equilibration and are consistent with regional isotherms based on calcite-dolomite solvus thermometry (Sobol, 1973; Sobol and Essene, 1973; fig. 1) and garnet-biotite Fe-Mg exchange thermometry (Rathmell, Essene, and van der Pluijm, in submission). In subsequent discussion, a temperature of 485°C is assumed for the peak of regional metamorphism near the Tudor gabbro.

No aluminosilicate polymorphs have been observed in the vicinity of the Tudor gabbro; however Carmichael (1970) mapped a kyanite-sillimanite isograd 10 km to the west near Whetstone Lake (fig. 1). Intersection of the kyanite-sillimanite transition with the 500° to 525°C isotherms of Sobol (1973) indicate a pressure near 4 kb (Holdaway, 1971). This pressure has been assumed for the Tudor area as well.

Contact Metamorphism

Peak temperatures of contact metamorphism associated with intrusion of the Tudor gabbro have been determined using calcite-graphite carbon isotope geothermometry (Dunn and Valley, 1992). The temperature dependence of ^{13}C distribution between calcite and graphite has been empirically calibrated (Valley and O'Neil, 1981; Wada and Suzuki, 1983; Dunn and Valley, 1992; Kitchen and Valley, 1995). Application of this system at Tudor yields good agreement with solvus temperatures for samples away from the contact, but temperatures within 1.5 km of the gabbro are significantly higher than 500°C, rising systematically toward the contact. Temperatures within the marble were ~730°C immediately adjacent to the pluton and decrease with distance from the contact (fig. 4). The 700°, 600°, and 550° isotherms are located approx 150, 750, and 1500 m from the pluton, and temperatures of ~485° (indistinguishable from the regional metamorphism) are indicated at 2 km and more from the pluton (fig. 4). The good correlation of calcite-graphite temperature with distance to the gabbro contact indicates that these high temperatures reflect the earlier contact metamorphism and were not reset during lower amphibolite facies metamorphism. The later regional metamorphism did not reset the calcite-graphite isotopic system, because carbon diffusion is very slow in graphite, and, once formed, it resists further isotopic exchange (Valley and O'Neil, 1981; Dunn and Valley, 1992; Kitchen and Valley, 1995).

The temperature gradient determined from calcite-graphite isotope thermometry is consistent with the thermal consequences of the intrusion if the ambient temperature of the country-rock was 250° to 300°C at the time of gabbro emplacement (Jaeger, 1959, 1964), assuming a cylindrical intrusion at 1150° to 1200°C (contacts are essentially vertical). This ambient temperature, combined with typical crustal densities and a geothermal gradient of 25°/km, suggests a pressure of 3 to 4 kb at the time of contact metamorphism. A higher intrusion temperature and/or geothermal gradient would allow a lower pressure estimate; however the temperature-fluid composition relations at 4 kb discussed in the next

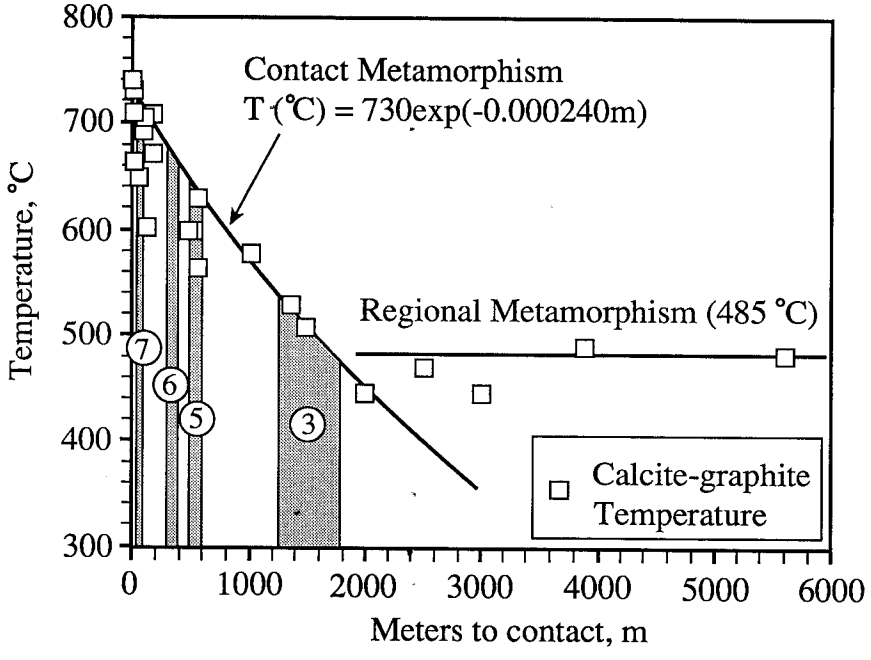

Fig. 4. Contact metamorphic temperature gradient discerned from calcite-graphite thermometry (open boxes, Dunn and Valley, 1992) and observed positions of isograds 3, 5, 6, and 7.

section are consistent with the reaction positions around the intrusion. Lower pressures would require correspondingly lower contact metamorphic temperatures, and these would be at odds with the calcite-graphite thermometry. Thus, it appears likely that these rocks occupied mid-crustal levels from the time of mafic plutonism (~ 1.24 Ga) until at least the time of major regional metamorphism (~ 1.10 Ga). This is reasonable given the long protracted history of the Grenvillian Orogeny (Easton, 1986; Lumbers and others, 1990; Mezger and others, 1993).

PHASE EQUILIBRIA

Idealized T-X(CO_2) Relations

The T–X(CO_2) relations of pertinent reactions at 4 kb are shown in figure 5 based on the thermodynamic data set of Berman (1988) and using the Redlich-Kwong equations of Kerrick and Jacobs (1981) for H_2O-CO_2 mixing. The equilibria calculations assume a binary H_2O-CO_2 fluid. This assumption is supported by calculation of the molar proportions of fluid species present during metamorphism. Many marble samples contain graphite (carbon activity = 1) which allows the relative propor-

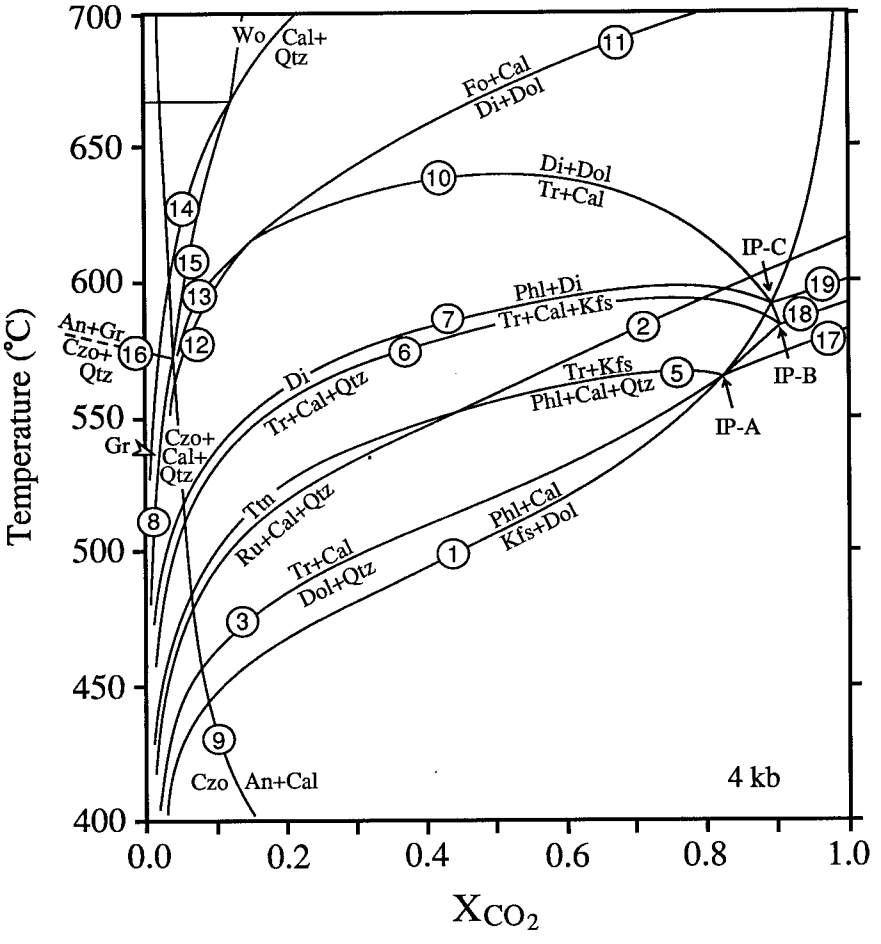

Fig. 5. T-X(CO_2) diagram at 4 kb showing the positions of end-member reactions pertinent to metamorphism of marble in the Tudor area based on the thermodynamic data set of Berman (1988). Reactions are numbered as in table 1. Some reactions are omitted for clarity. Invariant points A, B, and C are indicated.

tions of fluid species in the C–O–H system to be determined. Lamb and Valley (1984, 1985) show that CH_4 is the only fluid species other than CO_2 and H_2O of volumetric importance at the metamorphic conditions of interest. At 500°C and 4 kb, values of $X(CO_2)$ = 0.010, 0.020, and 0.030 correspond to $X(CH_4)$ = 0.012, 0.0064, and 0.0046, respectively, and log $f(O_2)$ = −24.0, −23.7, and −23.5, respectively, (Lamb, 1987) which are 0.2 to 0.7 log units below FMQ at 4 kb (Meyers and Eugster, 1983). Thus, CH_4 is not a major constituent of the metamorphic fluid in this study.

T-X(CO_2) Relations Adjusted for Solid Solution

Marble.—Isobarically univariant reactions, as in figure 5, become polyvariant in natural systems with additional components. The compositions of minerals in selected samples (table 3) have been used to constrain the equilibrium conditions for the localities shown in figure 2 (details are given in app. 1). These samples were selected because they contain appropriate mineral assemblages and mineral compositions representative of those in the marble in general.

Low variance assemblages are uncommon in Tudor marbles. The equilibrium conditions for representative marble samples that do have low variance assemblages have been determined, constraining minimum or maximum values of X(CO_2) for univariant assemblages (samples 63, 98, 148, 175) and a specific X(CO_2) for one invariant assemblage (sample 110). These results provide an estimate of the T-X(CO_2) relations that correspond to reactions 5, 6, 7, 8, and 9 in Tudor marbles. Biotite and amphibole analyses (Allen, 1976) similarly constrain T-X(CO_2) relations for reactions 1 and 3. The methods and details of constraining mineral-fluid conditions for the selected samples are given in app. 1, and the results are summarized in table 4 and figures 6 and 7.

The preserved equilibria indicate that the X(CO_2) of the fluid in marble decreased toward the Tudor gabbro becoming very H_2O-rich at the contact. Biotite-bearing marble on the low-grade side of the amphibole + calcite isograd (isograd 3) had X(CO_2) > 0.28 at 485°; for marble at the amphibole + calcite isograd, X(CO_2) = 0.25 to 0.28 at 485°C (fig. 6). Sample 98, on isograd 5 (amphibole + K-feldspar), requires X(CO_2) = 0.025 at 485°C and X(CO_2) > 0.014 regardless of temperature (fig. 7). Sample 148 lies close to but on the low-grade side of isograd 6 and is constrained by reaction 9 to X(CO_2) = 0.012 at 485°C and to X(CO_2) > 0.010 at all temperatures (fig. 7). Samples 63 and 175, both on or within isograd 7, require X(CO_2) of 0.004 and 0.006, respectively, at 485°C and X(CO_2) < 0.0045 and 0.012, respectively, regardless of temperature (fig. 7). Sample 110 is located in an area dominated by siliceous metasedimentary rocks coincident with a localized metamorphic high (fig. 2). This sample constrains X(CO_2) to 0.014 and temperature to 435°C. Thus, samples 98, 110, and 148 require a higher X(CO_2) than samples 63 and 175, and the H_2O content of metamorphic pore fluids increased toward the gabbro.

Reaction 14, the wollastonite-forming reaction, places an additional T–X(CO_2) constraint on the Tudor marbles. Calcite + quartz assemblages are common throughout these marbles even at the contact, and wollastonite has not been found in spite of a directed search (58 samples within 100 m of the contact; Dunn, ms). Allen (ms) reports wollastonite in a marble xenolith within the gabbro, but none within the contact aureole. The absence of wollastonite requires X(CO_2) greater than 0.004 at 485°C and greater than 0.20 at 700°C.

Marble equilibria also place constraints on metamorphic temperatures (figs. 6 and 7). Sample 98 requires temperatures above 460° and

below 627°C, samples 148 and 175 indicate temperatures below ~525°C, and sample 63 requires temperatures at or below ~485°C. Sample 110 restricts temperature to 435°C. The absolute errors in these temperature restrictions and in the $X(CO_2)$ determinations are difficult to assess because there are uncertainties in the mineral analyses, activity models, thermochemical data, and extrapolation to the pressures and temperatures of interest. The geothermometry results discussed earlier are more accurate determinants of temperature conditions than the mineral fluid equilibria. Nevertheless, the general agreement of equilibrium restrictions with a regional metamorphic temperature of 485°C confirms the methods applied.

Gabbro.—A compositional gap is seen in sodic feldspars within metagabbro samples indicating that equilibration was below the crest of the peristerite solvus. Most metagabbro samples contain albite (~An2-4); however, four were found to contain oligoclase (An19-25), and one contains coexisting albite (An2.3) and oligoclase (An19.1) which approximates the limbs of the peristerite solvus at 4 kb and ~500°C (Smith, 1983). Thus phase relations in metagabbro, as in marble, reflect the regional metamorphic conditions.

The oligoclase in these metagabbro samples coexists with epidote + calcite. The T-$X(CO_2)$ relations for these are constrained by reaction 9 to very H_2O-rich conditions. Values of K_9 range from 3.8 to 10.7 which correspond to an $X(CO_2)$ of 0.005 to 0.014 at 485°C (fig. 7).

MINERAL REACTION AND FLUID HISTORY OF MARBLE

The metamorphic fluid-rock interactions in the marble adjacent to the Tudor gabbro have been investigated by considering various reaction pathways for the representative samples described above and for two idealized marble protoliths. The fluid-mineral equilibria during metamorphism is assumed to have been governed by the T-X relations determined for the representative samples in the previous section. The idealized marble protoliths include a minimum-reaction assemblage, "Marble 1", and a maximum-reaction assemblage, "Marble 2", conceived to represent a range of the marble compositions in the field area (table 5).

No-Infiltration Model

First, we consider "no-infiltration" models for contact metamorphism of the idealized marble protoliths. These simulations allow mineral reactions to proceed in response to heating with expulsion of the fluids produced, but no fluid enters the rock undergoing reaction. Fluid produced in adjacent rocks is thus assumed to rise in the crust without interacting with marble. Building on the pioneering work of Greenwood (1975), a closed-system, no-infiltration model was proposed by Rice (1977) to explain the mineral reaction zones in the Marysville aureole, Montana. No-infiltration models discussed by Ferry (1991) and Ferry and Dipple (1992) are essentially equivalent to the low porosity case employed below.

TABLE 3

Mineral compositions within selected samples

	Plagioclase							K-feldspar		
Sample	98	110	148	238	237	220	202	98	110	148
SiO_2	61.26	63.61	61.48	62.56	61.07	63.14	63.25	64.69	64.24	62.88
Al_2O_3	23.70	22.72	24.29	22.82	24.61	23.92	23.28	17.76	18.20	20.42
Fe_2O_3	0.06	0.02	0.05	0.15	0.08	0.08	0.26	0.05	0.11	0.04
CaO	5.91	4.37	5.38	4.37	5.39	4.58	4.11	0.06	0.08	0.07
Na_2O	8.18	8.91	8.49	9.43	8.87	9.31	9.58	0.04	0.34	0.65
K_2O	0.05	0.32	0.14	0.06	0.07	0.06	0.05	17.12	16.13	16.18
Total	99.16	99.95	99.83	99.39	100.09	101.09	100.53	99.72	99.10	100.24
	normalized to 5 cations									
Si	2.747	2.820	2.732	2.778	2.697	2.759	2.776	3.005	3.000	2.885
Al	1.253	1.187	1.271	1.194	1.281	1.232	1.204	0.973	1.001	1.104
Fe^{3+}	0.002	0.001	0.002	0.005	0.003	0.003	0.009	0.002	0.004	0.002
Ca	0.284	0.208	0.256	0.208	0.255	0.214	0.193	0.003	0.004	0.003
Na	0.711	0.766	0.731	0.812	0.760	0.789	0.815	0.003	0.031	0.059
K	0.003	0.018	0.008	0.003	0.004	0.003	0.003	1.014	0.960	0.947

	Clinozoisite/epidote								Garnet
Sample	110	148	63	175	238	237	220	202	175
SiO_2	38.44	39.24	39.23	38.74	38.17	39.34	38.14	38.42	39.69
Al_2O_3	28.35	29.19	32.13	26.07	30.75	31.66	27.06	28.27	21.77
Fe_2O_3	6.65	5.13	1.41	8.92	4.47	2.96	8.71	7.59	1.28
MgO	0.05	0.06	0.00	0.05	0.02	0.04	na	0.02	0.02
CaO	23.21	24.21	24.37	23.82	23.74	24.05	23.23	23.37	37.11
MnO	0.52	0.00	0.02	0.06	0.11	0.06	0.14	0.14	0.06
TiO_2	na	0.02	0.00	0.04	0.07	0.05	0.00	0.03	0.03
Cr_2O_3	na	na	na	0.03	na	na	na	na	0.03
H_2O*	1.92	1.94	1.95	1.91	1.94	1.96	1.90	1.92	
Total	99.14	99.79	99.11	99.64	99.27	100.12	99.18	99.74	99.99
	normalized to 8 cations								
Si	3.001	3.029	3.009	3.042	2.954	3.002	3.003	2.994	2.990
Al	2.607	2.661	2.905	2.414	2.805	2.849	2.512	2.597	1.932
Fe^{3+}	0.389	0.298	0.081	0.526	0.260	0.170	0.516	0.445	0.073
Mg	0.003	0.007	0.000	0.005	0.002	0.005	na	0.002	0.003
Ca	1.940	2.003	2.003	2.005	1.968	1.967	1.960	1.951	2.994
Mn	0.060	0.000	0.002	0.004	0.007	0.004	0.009	0.009	0.004
Ti	na	0.002	0.000	0.002	0.004	0.003	0.000	0.002	0.002
Cr	na	na	na	0.002	na	na	na	na	0.002
OH*	1.000	1.000	1.000	1.000	1.000	1.000	1.000	1.000	

	Biotite			Amphibole				Cpx
Sample	98	110	63	98	110	148	63	63
SiO_2	39.57	38.28	40.42	54.86	50.25	54.62	44.10	51.60
Al_2O_3	16.47	16.28	14.78	2.67	5.38	1.32	12.20	3.51
FeO	11.01	14.57	6.90	7.92	12.70	12.19	6.48	4.47
MgO	16.70	14.26	21.61	18.47	14.12	15.99	16.34	14.08
CaO	0.13	0.16	0.00	13.10	12.55	12.91	12.11	23.93
MnO	0.03	0.04	0.07	0.04	0.00	0.07	0.06	0.21
TiO_2	0.69	0.77	0.23	0.06	0.19	0.05	1.00	0.59
Na_2O	0.07	0.00	0.14	0.32	0.69	0.18	2.96	0.83
K_2O	9.92	9.98	10.17	0.14	0.45	0.12	1.09	na
F	1.53	1.36	1.77	0.43	0.38	0.43	0.50	na
H_2O*	3.31	3.30	3.29	1.92	1.86	1.88	1.82	
Total**	98.79	98.43	98.64	99.75	98.41	99.58	98.45	99.22
	cation normalized***							
Si	2.958	2.928	2.946	7.732	7.390	7.863	6.437	1.903
Al^{IV}	1.042	1.072	1.054	0.268	0.610	0.137	1.563	0.097
Al^{VI}	0.410	0.396	0.216	0.176	0.323	0.087	0.537	0.056
Fe^{2+}	0.688	0.932	0.421	0.934	1.562	1.468	0.791	0.138
Mg	1.861	1.625	2.347	3.880	3.095	3.431	3.555	0.775
Ca	0.010	0.013	0.000	1.978	1.978	1.992	1.894	0.947
Mn	0.002	0.003	0.004	0.005	0.000	0.009	0.007	0.007
Ti	0.039	0.044	0.013	0.006	0.021	0.005	0.110	0.017
Na	0.010	0.000	0.020	0.087	0.197	0.050	0.838	0.060
K	0.946	0.974	0.946	0.025	0.084	0.022	0.203	na
F	0.349	0.318	0.398	0.192	0.177	0.196	0.231	na
OH*	1.651	1.682	1.602	1.808	1.823	1.804	1.769	

TABLE 3

(continued)

Sample	Calcite 98	110	148	175
CaO	53.81	55.29	55.26	56.10
MgO	0.60	0.14	0.18	0.05
FeO	0.65	0.33	0.36	0.07
MnO	0.06	0.07	0.03	0.09
CO_2*	43.33	43.78	43.80	44.20
Total	98.45	99.61	99.63	100.51
	normalized to 2 cations			
Ca	1.949	1.982	1.980	1.992
Mg	0.031	0.007	0.009	0.003
Fe	0.018	0.009	0.010	0.002
Mn	0.002	0.002	0.001	0.003
C*	2.000	2.000	2.000	2.000

* Calculated by stoichiometry.
** Adjusted for F ≡ O.
*** Biotite analyses normalized to 7 cations (excluding Ca, Na, K), amphibole to 13 cations (excluding Ca, Na, K), and clinopyroxene to 4 cations.
na = not analyzed.
All Fe as Fe_2O_3 in feldspars, clinozoisite/epidote, and garnet.
All Fe as FeO in biotite, amphibole, clinopyroxene, and calcite.

TABLE 4

Metamorphic fluid compositions for selected marble and gabbro samples

	Constraining assemblage*	Equilibria restrictions**	$X(CO_2)$; T (°C)
MARBLE			
Further from gabbro than isograd 3***	Bi + Cal	$K_1 \geq 0.17$	≤0.69; 485°
Isograd 3***	Am + Cal + Dol + Qtz	$0.29 \leq K_3 \leq 0.51$	0.25–0.28 @ 485°
Sample 98	Bi + Cal + Qtz + Am + Kfs + An	$K_5 = 64.1$, $K_9 \leq \sim 4.29$	≥0.014; =0.025 @ 485°
Sample 110	Bi + Cal + Qtz + Am + Kfs + An + Czo	$K_5 = 2.98$, $K_9 = 5.57$	=0.014; 435°
Sample 148	Am + Cal + Qtz + Kfs + An + Czo	$K_{14} < 1$, $K_9 = 4.29$	≥0.010; ≤525°
Isograd 6†	Am + Cal + Qtz + Cpx	$K_6 = 13.5$	0.10 @ 485°
Sample 63	Am + Cal + Cpx + Bi + Czo + Ab	$K_7 \geq 1{,}790$, $K_9 \geq 16.6$, $K_{14} < 1$	≥0.0045; ≤485°
Sample 175	Grt + Czo + Cal + Qtz + Ab	$K_8 = 4.17$, $K_9 \geq 3.75$, $K_{16} \leq 0.178$	≤0.012; ≤520°
GABBRO			
Sample 238	Czo + An + Cal	$K_9 = 10.7$	0.005; 485°
Sample 237	Czo + An + Cal	$K_9 = 5.90$	0.009; 485°
Sample 220	Czo + An + Cal	$K_9 = 3.81$	0.014; 485°
Sample 202	Czo + An + Cal	$K_9 = 7.65$	0.007; 485°

* Mineral abbreviations as in table 1.
** Equilibrium constants, K_i for reaction i, solids only (see app. 1).
*** Data from Allen, 1976.
† Assuming Tr and Di activities from sample 63.

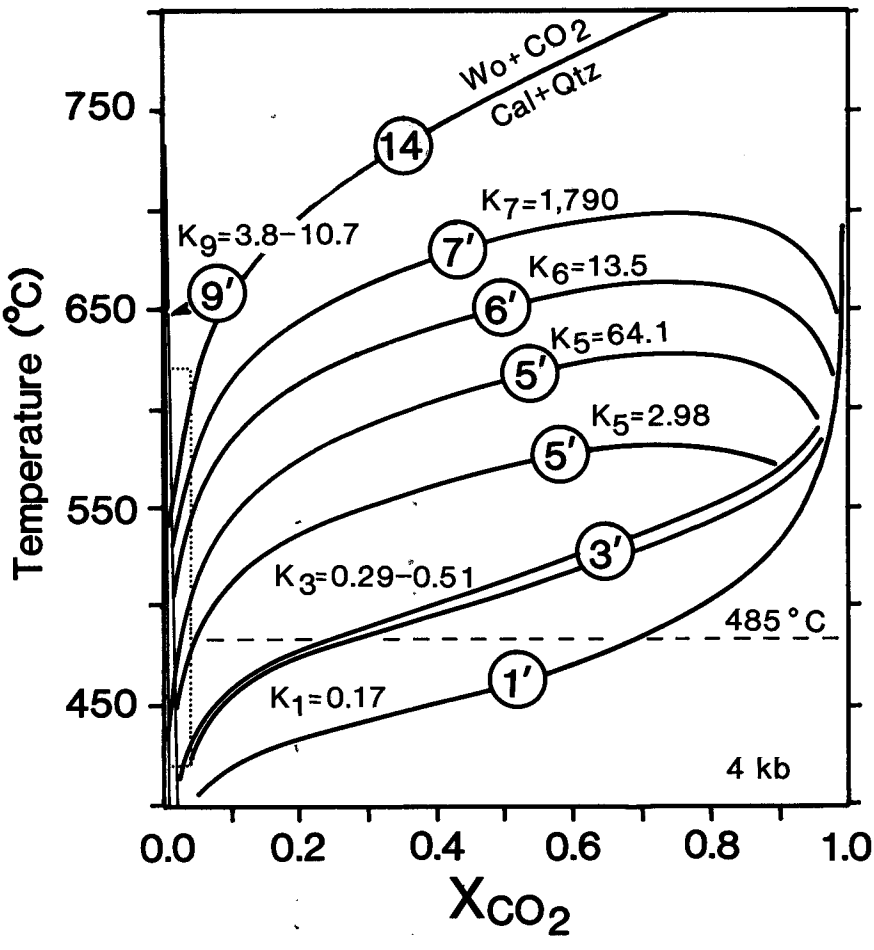

Fig. 6. T-X diagram at 4 kb showing the positions of selected equilibria adjusted for mineral solid solutions. Reaction curves are positioned as appropriate for the equilibrium constants, K_i for reaction i, calculated for particular samples (table 4 and app.); reaction 14 is shown for endmember compositions. The position of reaction 9′ (K_9 = 3.8-10.7) corresponds to equilibria in metagabbro, all other curves apply to marble. The regional metamorphic temperature of 485°C is dashed for reference and the portion of T-X space expanded at low $X(CO_2)$ in figure 7 is shown in dotted outline.

The T-$X(CO_2)$ reaction pathway in this model depends on the porosity of the rock and the manner in which fluid is expelled. Two cases are considered, one with low porosity (0.01 percent) and one with rather high porosity (1.0 percent). In both cases the pore space is initially occupied by water-rich fluid ($X(CO_2)$ = 0.20) at 4 kb and an initial temperature less than 400°C. For these models, the fluids produced by a

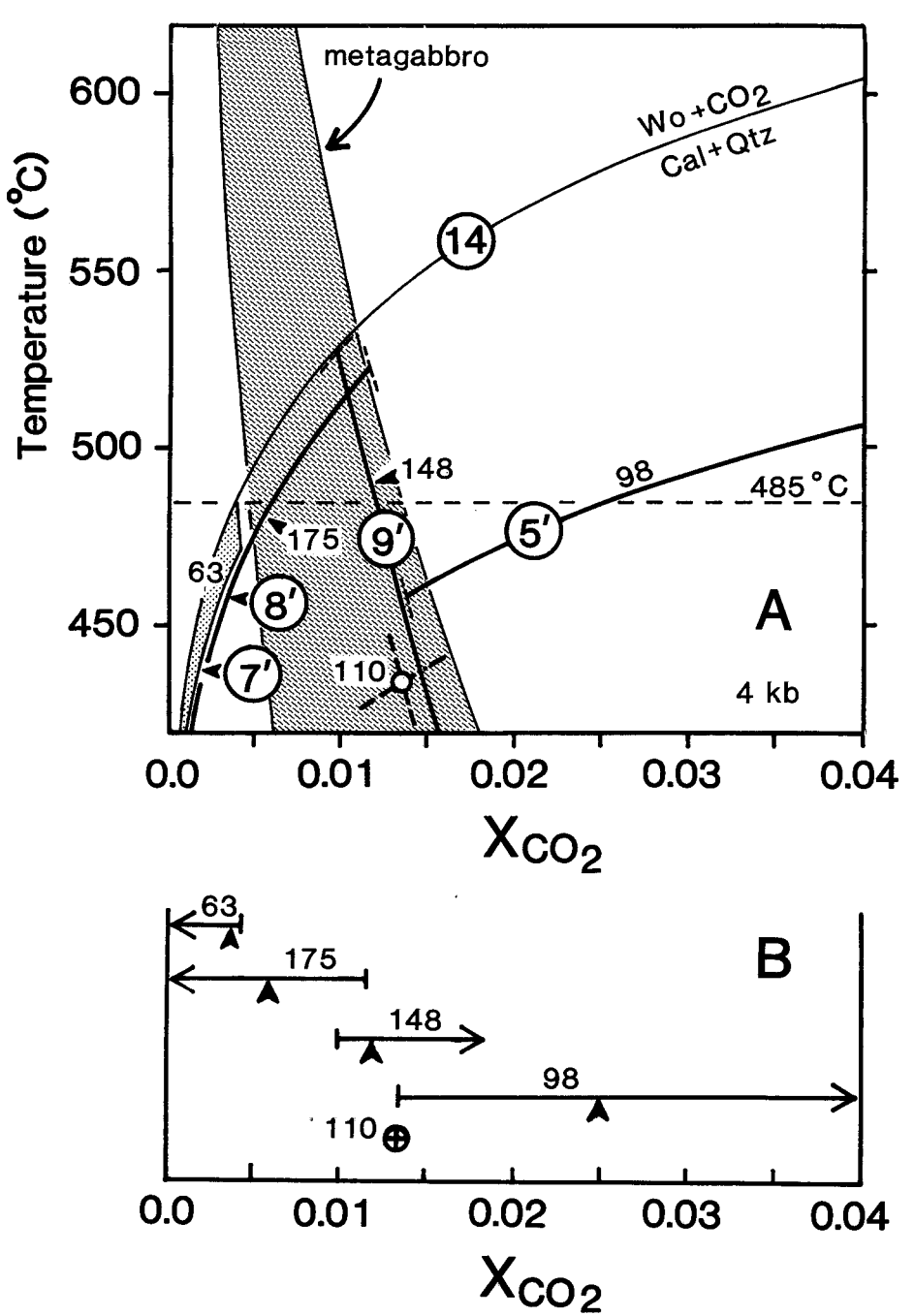

Fig. 7(A) T-X relations adjusted for solid solution at H_2O-rich conditions. Samples are constrained by equilibria as described in the app. Marble samples 98, 148, and 175 lie on adjusted reaction curves, sample 110 plots at the intersection of adjusted reactions 5 and 9 and sample 63 is constrained to lie within the stippled area. Metagabbro samples are restricted by equilibrium 9 to the patterned area indicated and show that the fluid composition of metagabbro samples during regional metamorphism are similar to that of marble near the contact. Samples 63, 110, 148, and 175 have reequilibrated during regional metamorphism as their present equilibria are incompatible with the elevated temperatures (> 525°C) of contact metamorphism. (B) Ranges of $X(CO_2)$ permitted by phase equilibria for marble samples. Arrow heads correspond to regional metamorphism at 485°C.

TABLE 5

Model parameters and reaction products for fluid flux calculations discussed in text. Marbles 1 and 2 represent "minimum-reaction" and "maximum-reaction" lithologies typical of marbles at Tudor*

Mineral modes	Cal**	Dol	Qtz	Phl	Kfs	Tr	Di
Marble 1 (initial)	88.0	6.0	4.0	0.0	2.0	0.0	0.0
After Reaction 1	90.8	2.5	4.0	2.7	0.0	0.0	0.0
After Reaction 3	92.5	0.0	2.7	2.7	0.0	2.1	0.0
After Reaction 5	92.1	0.0	0.6	0.0	2.1	5.2	0.0
After Reaction 6	91.8	0.0	0.0	0.0	2.1	1.5	4.6
After Reaction 7	91.7	0.0	0.0	0.3	1.9	0.0	6.1
Total volume loss = 3.9 percent							
Marble 2 (initial)	61.0	22.0	13.0	0.0	4.0	0.0	0.0
After Reaction 1	66.2	15.1	13.2	5.5	0.0	0.0	0.0
After Reaction 3	75.6	0.0	5.0	5.8	0.0	13.6	0.0
After Reaction 5	74.7	0.0	0.6	0.0	4.4	20.3	0.0
After Reaction 6	74.2	0.0	0.0	0.0	4.4	16.7	4.7
After Reaction 7	72.7	0.0	0.0	2.3	3.1	0.0	21.9
Total volume loss = 13.3 percent							

Reaction IP-A: $8Qtz + 0.444Cal + 1.556Dol + 1.148Phl = Tr + 1.148Kfs + 0.148H_2O + 3.556CO_2$.
Reaction IP-B: $1.7143Qtz + 0.1071Cal + 0.8214Dol + 0.0357Tr = Di + 0.0357H_2O + 1.75CO_2$.
Reaction IP-C: $0.383Cal + 1.872Dol + 1.128Tr + Kfs = Phl + 4.511Di + 0.128H_2O + 4.128CO_2$.
dT/dz (degrees/cm) for horizontal flow, $-0.001752\exp(-0.00000240z)$.
Reaction 1: $X(CO_2) = -38.5265 + 0.216539T - 4.32313(10^{-4})T^2 + 3.67638(10^{7})T^3 - 1.09693(10^{-10})T^4$, T = 420 to 560°C.
Reaction 3: $X(CO_2) = 342.491 - 2.56076T + .00709927T^2 - 8.65207(10^{-6})T^3 + 3.92024(10^{-9})T^4$, T = 450 to 590°C.
Reaction 5: $X(CO_2) = 2.99376(10^{-7})\exp(0.0233095T)$, T = 450 to 625°C.
Reaction 6: $X(CO_2) = 8.85456(10^{-8})\exp(0.0239007T)$, T = 450 to 650°C.
Reaction 7: $X(CO_2) = 1.15933(10^{-7})\exp(0.0222730T)$, T = 450 to 695°C.

* Reaction products pertain to the "up-temperature flow" and "flow outward from the contact" models.

** Percentage of calcite is 1 percent lower in high-porosity models to accomodate 1 percent porosity.

given reaction mix with that present in the pore space until the fluid volume exceeds the porosity by 1 percent (1 percent of the porosity). At that point a small amount of fluid is expelled to bring the fluid volume back down to its initial volume. In this way, the composition of the pore fluid (as well as the expelled fluid) changes as reactions proceed incrementally. Molar volumes for CO_2 and H_2O (at 4 kb, 500°C, from Shmonov and Shmulovich, 1974, and Burnham, 1969, respectively) were assumed constant for these calculations. Adjusting fluid volumes for changing temperature has negligible effects on the results.

The fluid volume, V_{fl}, and fluid composition, $X(CO_2)$, are given by

$$V_{fl} = V(CO_2)[n(CO_2) + \nu(CO_2)\xi'] + V(H_2O)[n(H_2O) + \nu(H_2O)\xi'] \quad (1)$$

and

$$X(CO_2) = \frac{n(CO_2) + \nu(CO_2)\xi'}{n(CO_2) + \nu(CO_2)\xi' + n(H_2O) + \nu(H_2O)\xi'} \quad (2)$$

where V(i) is the molar volume of fluid i, n(i) is the number of moles of fluid i present before an increment of reaction, and ν(i) is the stoichiometric coefficient of fluid i in the reaction. The reaction progress in moles for each increment, ξ', is selected such that V_{fl} will exceed the initial porosity by 1 percent. After each increment, the fluid volume is reduced proportionately so as to maintain the current $X(CO_2)$ and determine the new n(i) values for the next increment of reaction.

In these models, reaction 1 is encountered in the idealized marble protoliths when temperature reaches 435°C at which point phlogopite + calcite + CO_2 are produced at the expense of dolomite + K-feldspar + H_2O (fig. 8). This reaction proceeds step by step to invariant point A (fig. 8) where phlogopite is completely consumed by the invariant point reaction given in table 5. Further heating drives reaction 3 up to invariant point B where the pathways diverge depending upon the porosity and bulk composition (fig. 8).

In these simulations, the most conspicuous mineralogical changes occur by reaction at invariant points for the high-porosity case and at the CO_2-axis (reaction 18, dolomite + quartz out) for the low-porosity case (fig. 9). This model predicts that the tremolite-in and tremolite + K-feldspar-in isograds (isograds 3 and 5) will coincide (see also Greenwood, 1975; Rice, 1977; Rice and Ferry, 1982). These isograds are clearly separate in this study (fig. 3), and, therefore, this model does not describe the Tudor aureole. This model also fails to account for H_2O-rich conditions near the contact.

A corollary to this model which is similarly inapplicable is regional metamorphism alone without fluid infiltration. Regional metamorphism would follow the same reaction paths as shown above; however reaction would cease at 485°C without producing any of the reaction isograds above the phlogopite-in isograd.

H_2O-Rich Fluid Flow Outward from The Pluton

The H_2O-rich conditions indicated for metagabbro and marble samples at the contact are consistent with H_2O-rich fluid flow outward from the pluton into the country-rock during metamorphism. Such a process would result in a sequence of reaction zones concentric to the contact. The specific reactions would depend on whether the fluid flow occurred during contact metamorphism (in the presence of a thermal gradient) or during regional metamorphism (with an approximately constant temperature distribution).

H_2O infiltration during contact metamorphism.—The outward flow of H_2O-rich fluid during contact metamorphism would produce a sequence of reaction zones in the marble country-rock. The fluid composition

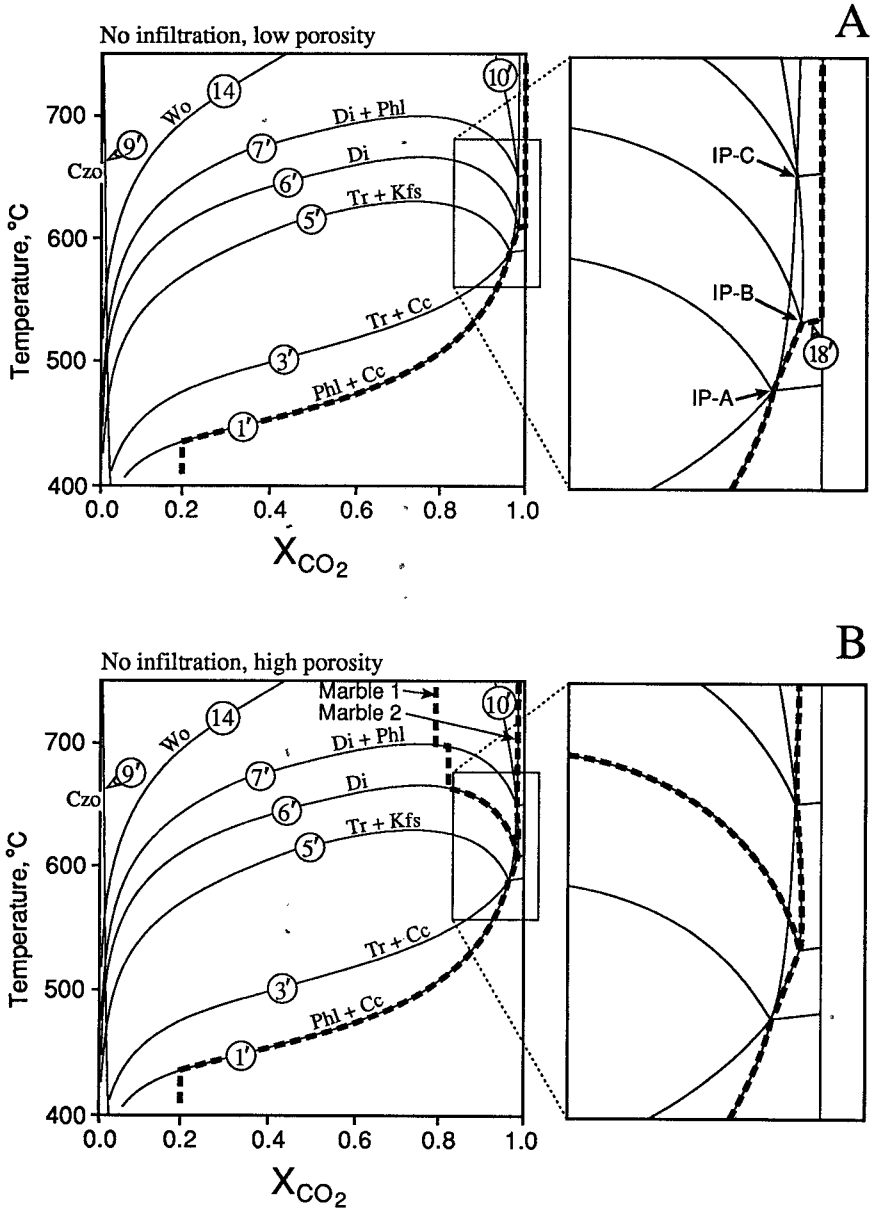

Fig. 8. Fluid reaction pathways for no-infiltration models discussed in text. The prime on a reaction number indicates adjustment for solid solutions (see text). (A) Inferred path for both idealized marble compositions assuming a low porosity, (B) inferred paths assuming high porosity.

along the flow path would be buffered at reaction fronts that migrate outward as flow continues. The infiltrating fluid at the contact would initially be out of equilibrium with quartz-bearing marble such that wollastonite would form via reaction 14 (quartz-absent marble is most abundant at high grades near the gabbro, but calcite + quartz assemblages are not uncommon). This and other reactions produce CO_2 which would dilute the H_2O–rich fluid in a step-wise fashion from one reaction to the next. The composition of fluid entering a reaction site would be determined by the last up-stream reaction. This type of process has been proposed for the Notch Peak contact aureole, Utah (Nabelek and others, 1984; Labotka, Nabelek, and Papike, 1988).

This reaction pathway is illustrated schematically in figure 10 which shows that wollastonite, not calcite + quartz, would be stable at elevated temperatures near the contact. The wollastonite-forming reaction can be applied in endmember form, because solid solutions are very limited in the reactants and products. The absence of wollastonite in the Tudor aureole precludes the infiltration of marble at the contact by H_2O-rich fluids during the peak temperatures of contact metamorphism.

Olivine is also absent in the Tudor contact aureole, although it is present within the marble xenolith mentioned earlier. Forsterite-forming reactions such as 11, 12, and 13 (fig. 5; table 1) are not included in figure 10 for simplicity, and because the appropriate activity of forsterite to apply is not known. However, the absence of olivine in the contact aureole, as with the absence of wollastonite, indicates that H_2O-rich fluid did not flow outward from the pluton during contact metamorphism.

H_2O infiltration during regional metamorphism.—As in the contact metamorphic case, the outward flow of H_2O-rich fluid during regional metamorphism would similarly produce a sequence of reaction zones in the marble country-rock, and the composition of the fluid along the flow path would be buffered at the point of reaction. This type of process has been described as a reaction front by Bickle and Baker (1990). If the fluid entering the flow path into the marble was pure H_2O, then one would again expect wollastonite at the contact just as in the case of H_2O infiltration during contact metamorphism. However, at the regional metamorphic temperature of 485°C, wollastonite is restricted to exceedingly H_2O-rich conditions, even more H_2O-rich than that indicated by epidote–oligoclase–calcite assemblages in metagabbro samples (fig. 7). Therefore, to simulate this model, the fluid infiltrating at the contact would have to be H_2O-rich enough to drive the diopside + phlogopite reaction (isograd 7, $X(CO_2) < 0.0045$), yet not so H_2O-rich as to form wollastonite ($X(CO_2) > 0.0035$). Thus, for modeling purposes, an initial fluid composition of $X(CO_2) = 0.0040$ is used.

This simulation assumes a horizontal column of marble 1 cm^2 in cross section extending outward from the contact at a uniform temperature of 485°C. Fluid of $X(CO_2) = 0.0040$ enters from the contact filling the available porosity in 1 cm^3 and displacing the fluid in each cm^3 down

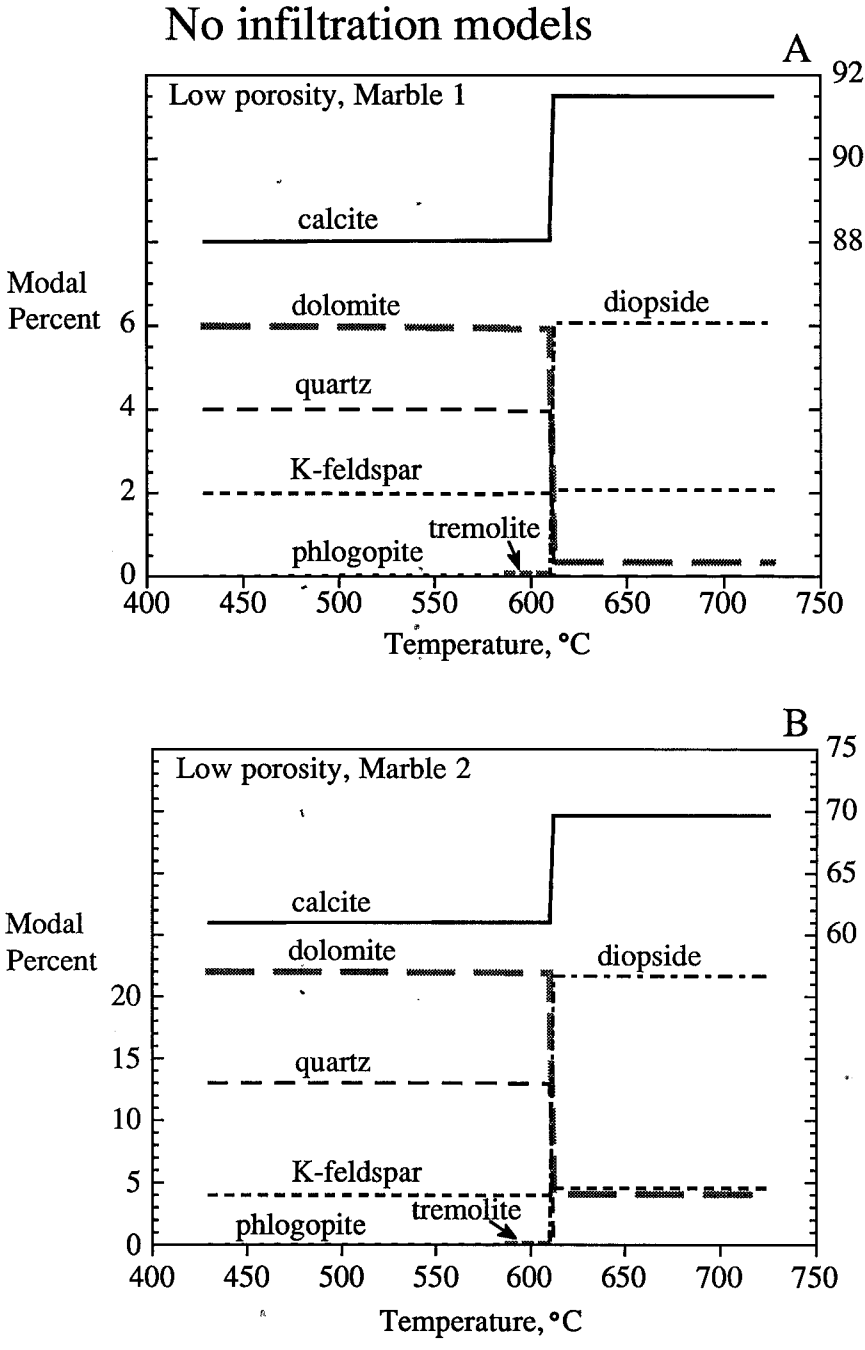

Fig. 9. Modal changes in idealized marble compositions (table 5) for no-infiltration models, (A, B) marble 1 and 2 assuming low porosity.

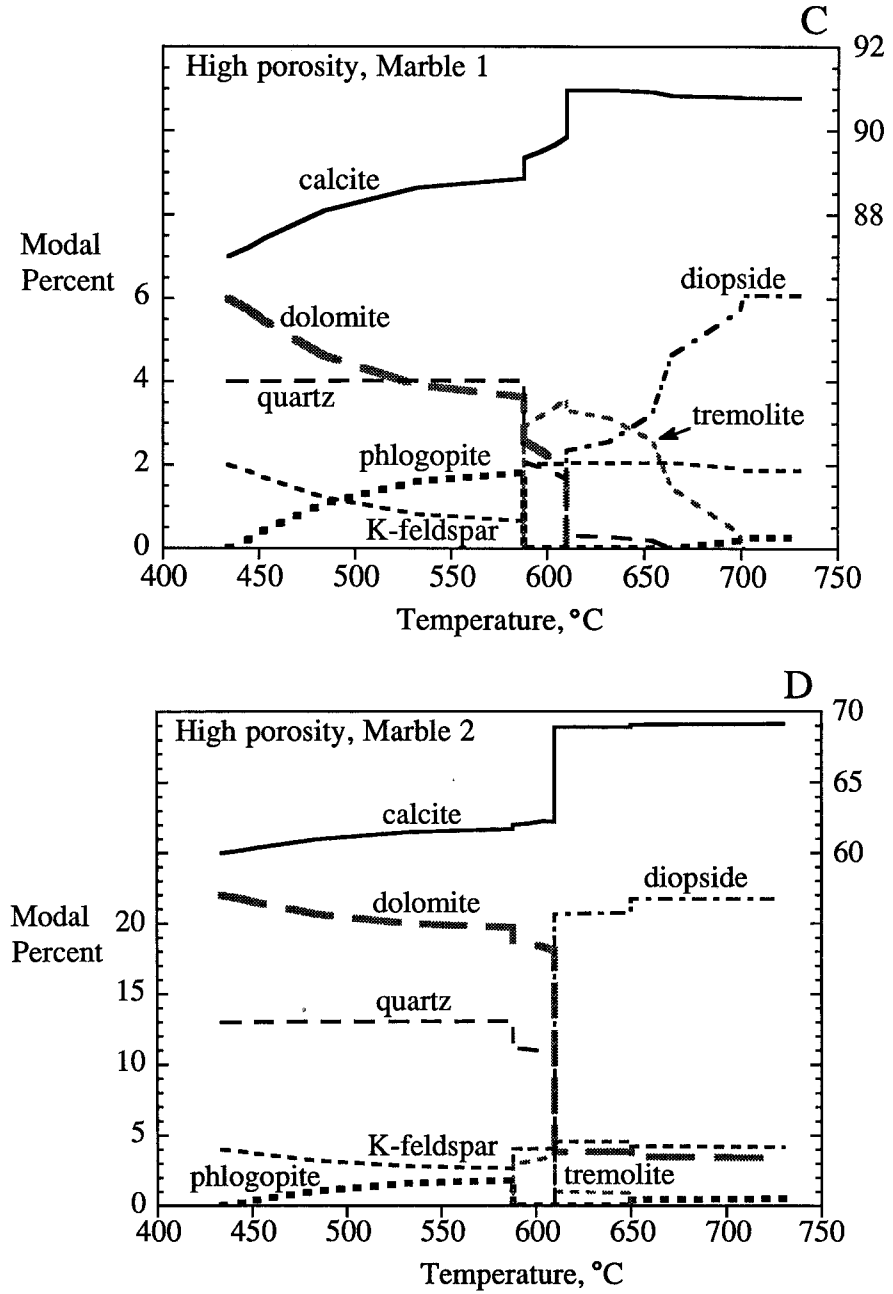

Fig. 9. (C, D) marble 1 and 2 assuming high porosity.

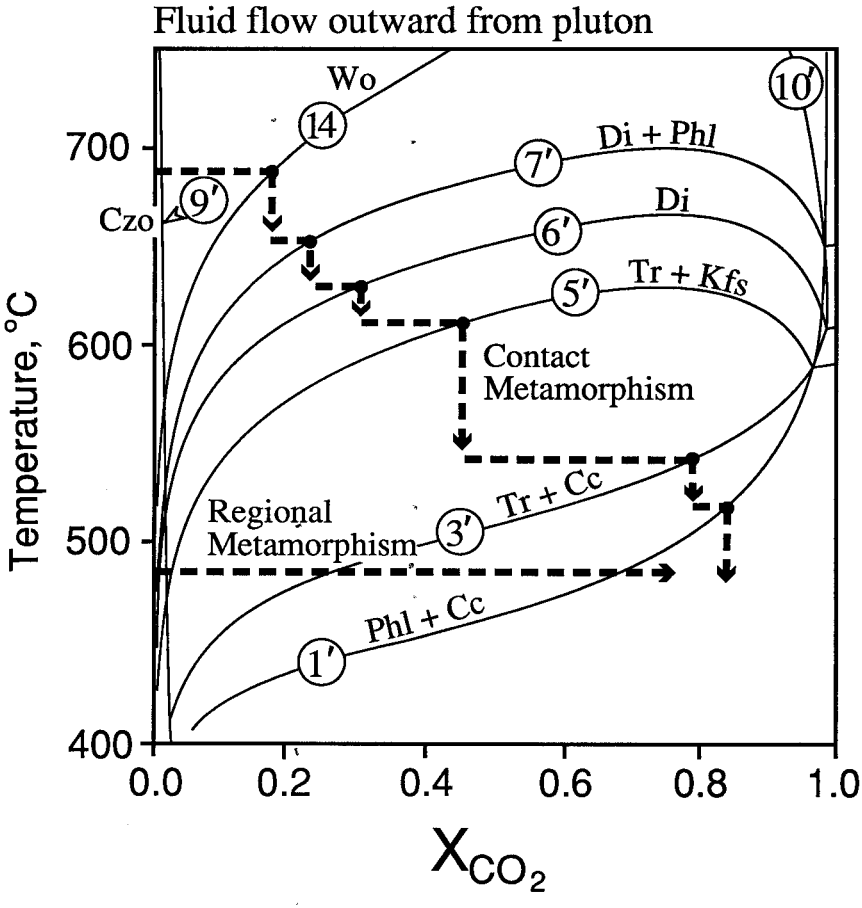

Fig. 10. Fluid reaction pathways for models of H_2O-rich fluids flowing outward from the gabbro contact during either contact metamorphism or regional metamorphism.

the column. Reactions proceed as necessary at reaction fronts where pore fluids are brought into equilibrium with the assemblages present, and then the process is repeated. Reactions occur only at discreet positions in the column as each reaction buffers the outgoing downstream fluid. This process is independent of porosity and the position of each reaction isograd depends only upon the initial rock mode, the composition of the infiltrating fluid, and the fluid flux. Fluid flux is monitored as "influx" at the column entrance and "outflux" at downstream positions. For marble 2, the outflux at the tremolite reaction, isograd 3, is 1.6 times the influx as a result of fluids produced by reactions, and the outflux outside the phlogopite + calcite reaction is 3.4 times the influx.

This model matches the observations at Tudor quite well in that it predicts discreet reaction zones with little or no overlap of reactant and product assemblages, distinct separation of the tremolite-in isograd and the tremolite + K-feldspar isograd, and decreasing X(CO2) toward the contact. Figure 11 illustrates the mineralogical changes in idealized marble 1 and 2 for influxes of 10^4 and 10^5 cm^3/cm^2, respectively. As well as this model predicts the observed mineral assemblages in the marble, it fails to acknowledge or include the contact metamorphism known to have occurred in response to the thermal effects of intrusion (for example, 730°C near the contact indicated by calcite-graphite thermometry).

Up-Temperature Fluid Flow

Another model to consider is fluid flow toward the pluton in the direction of increasing temperature during contact metamorphism. This model allows fluid buffering by each reaction until reactants are exhausted and then constant $X(CO_2)$ until the next reaction is encountered at a higher temperature further along the flow path. This type of reaction pathway is proposed for the Waits River formation, Vermont (Ferry, 1992), and for the Notch Peak contact aureole, Utah (Ferry and Dipple, 1992).

Baumgartner and Ferry (1991) show that for fluid flow along established temperature and pressure gradients with mineral-fluid equilibrium maintained along a flow path of length z, the time integrated molar fluid flux (q_m) is related to reaction progress (ξ), the temperature gradient (dT/dz), and the pressure gradient (dP/dz) along the flow path by the equation (see also Ferry, 1991 and Ferry and Dipple, 1991),

$$q_m = \frac{\nu_i \xi - X_i \sum_j (\nu_j \xi)}{[(\partial X_i/\partial T)_P(dT/dz) + (\partial X_i/\partial P)_T(dP/dz)]} \qquad (3)$$

where ν_i is the stoichiometric coefficient of fluid i in the reaction and X_i is the mole fraction of i in the fluid. When applied in well constrained circumstances, this relation yields not only quantities of fluid but also flow direction. In the case of nearly horizontal fluid flow, $(\partial X_i/\partial T)_P(dT/dz) \gg (\partial X_i/\partial P)_T(dP/dz)$, such that $(\partial X_i/\partial P)_T(dP/dz)$ can be ignored (assumed to equal zero). For $X_i = X(CO_2)$, which is always < 1, and for reactions that proceed left to right as written in table 1 (that is, ξ positive) the numerator of the equation will also be positive. Because $\partial X(CO_2)/\partial T$ is positive over the portion of interest of reactions 3 to 8 and fluid flux is taken to be positive in the direction z, dT/dz must also be positive, and thus, flow is indicated to be up-temperature (Baumgartner and Ferry, 1991; Ferry, 1991). This is schematically represented by the reaction path in figure 12.

This model predicts the position of a reaction as a function of fluid flux and reaction progress. If one assumes a contact metamorphic origin

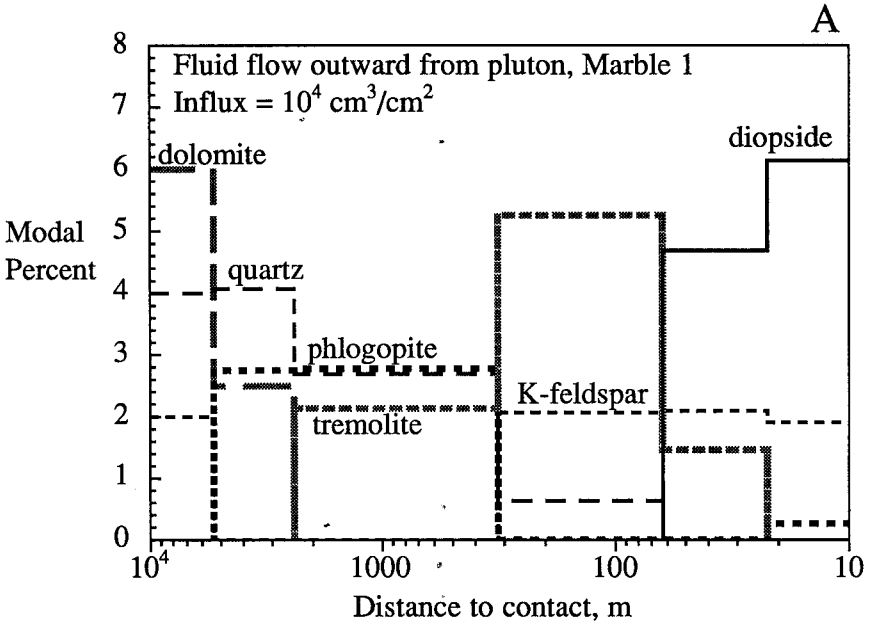

A.

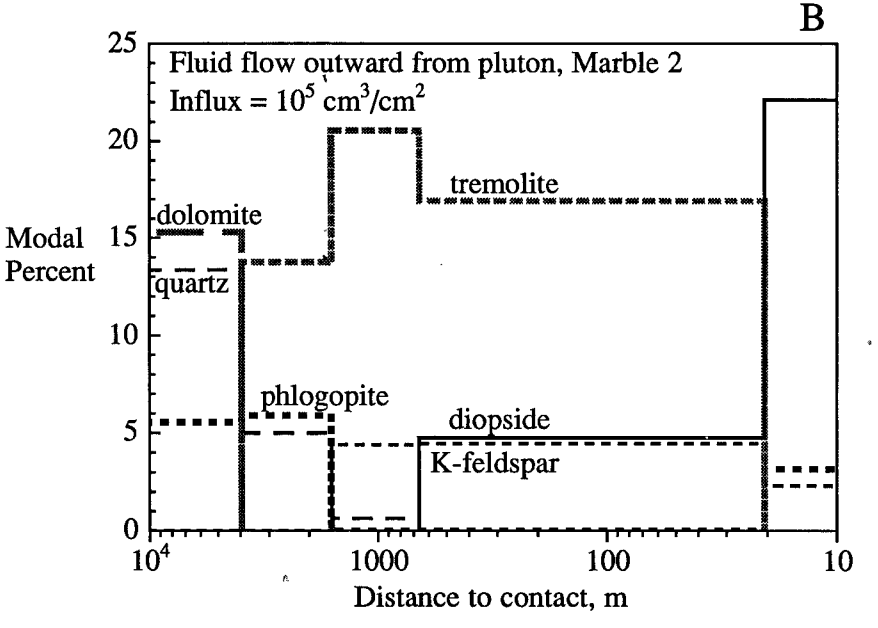

B.

Fig. 11. Modal changes in idealized marble 1 (A) and marble 2 (B) assuming H_2O-rich fluid flowing outward from the gabbro contact during regional metamorphism at 485°C.

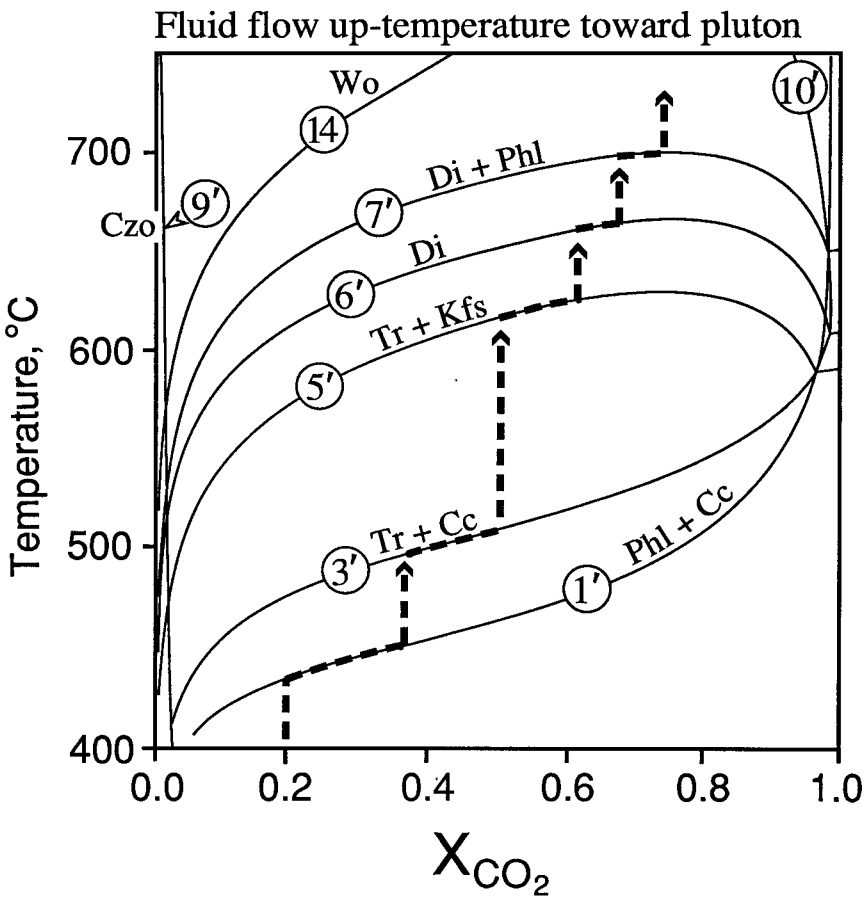

Fig. 12. Schematic fluid reaction pathway assuming up-temperature fluid flow during contact metamorphism.

for the isograds at Tudor, then the thermal gradient depicted in figure 4 can be used to assign a reaction temperature to each isograd. For the idealized marbles 1 and 2 and the appropriate model parameters for this study (table 5), model fluid fluxes of less than 100 moles/cm^2 are indicated for reactions 5 to 7 and 25 to 250 moles/cm^2 for reaction 3 (fig. 13). Reaction 1 cannot be quantified in this context because the regional metamorphic grade is above that reaction; thus the temperature of reaction is unknown. Reactions 5 to 7 exhibit thermal maxima in isobaric T-X(CO_2) space, and at Tudor these reactions proceeded near their maxima where X(CO_2) = 0.75. As $\partial X(CO_2)/\partial T$ approaches infinity near X(CO_2) values of 0.75 for these reactions, fluid flux becomes small, approaching zero. Of course, fluids produced by reaction must escape and, therefore, must flow from the reaction site, but non-reactive fluids

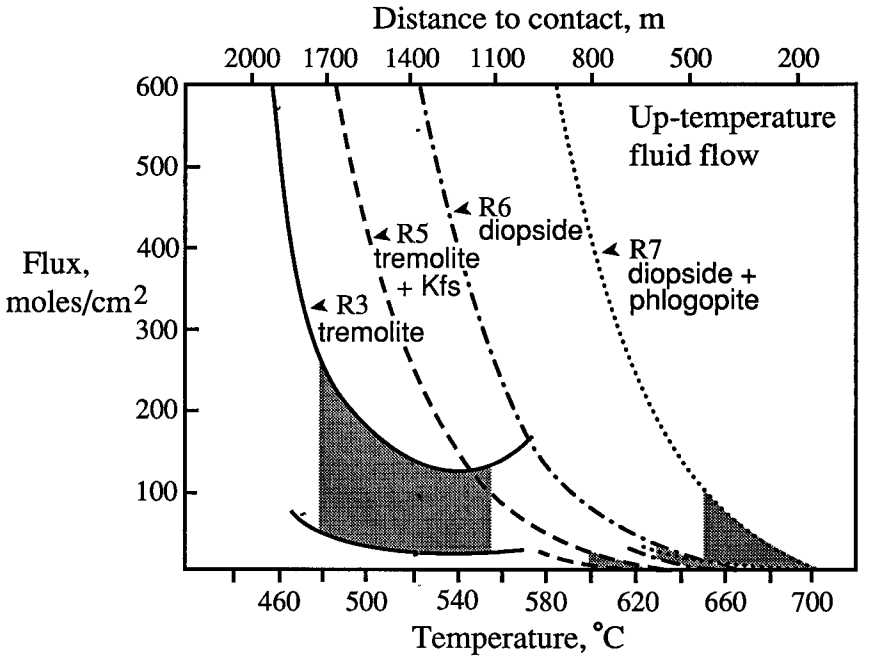

Fig. 13. Fluid fluxes corresponding to reactions 3, 5, 6, and 7 for up-temperature flow idealized marble 1 and 2. Only part of the curve for marble 1 is shown for clarity. The shaded regions correspond to the temperature and position of each isograd allowing for temperature uncertainties of ±30°C.

such as these do not affect reaction progress and are not identifiable in this situation.

Unlike reactions 5 to 7, reaction 3 has no thermal maximum. It does, however, have an inflection point near 500°C which, when considered in eq (3), produces a flux minima near 540°C (fig. 13). This is significant in that the position of the tremolite isograd (reaction 3) corresponds to a temperature of about 540°C or less which in turn corresponds to model fluxes of about 25 to 120 moles/cm^2 for this isograd. Up-temperature fluxes in this range would leave reaction 3 at $X(CO_2)$ values of 0.70 to 0.85. These fluid compositions correspond with the regions where $\partial X(CO_2)/\partial T$ is very large for reactions 5 to 7 restricting the model fluxes at these isograds to low values, less than 25 moles/cm^2. Therefore, no single flow path across the aureole is feasible in this model. Larger model fluxes are indicated for the outer aureole, and smaller model fluxes, approaching but not equal to zero, are indicated for the inner aureole.

This discrepancy between model fluxes for the inner and outer aureoles presents problems in portraying a mineral assemblage sequence for this model. However, the sequence would be consistent with the

reaction isograds. This model does not, however, predict the H_2O-rich conditions found near the contact.

Vertical Fluid Flow

Vertical downward flow is mechanically impossible at lithological pressures due to density influences and will not be considered, but upward flow is possible and expected (Walther and Orville, 1982). Upward vertical fluid flow is more complicated to model by eq (3) because, unless the geothermal gradient is inverted, $(\partial X_i/\partial T)\,(dT/dz)$ will be negative while $(\partial X_i/\partial P)\,(dP/dz)$ will be positive, and q_m depends on their relative values. As $(\partial X_i/\partial T)\,(dT/dz)$ generally dominates, forward mineral reaction in response to upward flow typically requires unusually low geothermal gradients ($dT/dP < \sim 15°/kb$). Reactions 5 to 7 exhibit pressure minima in isothermal P-$X(CO_2)$ space. At Tudor, these reactions proceeded at, or near, these minima where $X(CO_2) = 0.75$ and where $(\partial X(CO_2)/\partial P)$ becomes large, approaching infinity, such that the corresponding fluid flux becomes small, approaching zero. Again, fluid products must escape, but under these circumstances, they may be non-reactive.

Because reactions 5 to 7 proceeded at or near an $X(CO_2)$ of 0.75, they are consistent with small fluid fluxes whether flow was horizontal or vertical, and, either way, these reactions would have been driven mainly by increasing temperature. Reactions 3, 8, and 9 on the other hand, proceeded at values of $X(CO_2)$ different from that produced by reaction such that these reactions imply fluid flow.

Reaction 3 does not exhibit an isothermal pressure minima. Therefore, reaction due to vertical fluid flow would require an unusually low geothermal gradient (see above and also Ferry and Dipple, 1991). The geothermal gradient in the vicinity of an igneous intrusion will be highly dependent upon the geometry of the intrusion and vary greatly over the emplacement and cooling event. It is unlikely that a very low geothermal gradient would be sustained in such a setting, and, thus, vertical flow will not be considered as a plausible mechanism for production of isograd 3.

The Case for Polymetamorphism

Phase equilibria in marble around the Tudor gabbro indicate a complex history, and none of the simple "one metamorphism" models assessed thus far can adequately account for all of the observations at Tudor. The positions of isograds 3, 5, 6, and 7 can be explained by either up-temperature fluid flow during contact metamorphism or by flow of H_2O-rich fluid outward from the intrusion during regional metamorphism. However, the former model cannot account for the H_2O-rich conditions near the contact indicated by the presence of garnet (reaction 8) and clinozoisite (reaction 9), and the latter model fails to account for reactions that must have occurred during contact metamorphism. Only a polymetamorphic history for the Tudor contact aureole allows construc-

tion of a fluid-mineral reaction history that can account for all the observations at Tudor.

The occurrence of garnet (reaction 8) and clinozoisite (reaction 9) without wollastonite near the contact requires H_2O-rich conditions at temperatures below ~525°C. This clearly indicates that equilibria involving these phases became established after the peak of contact metamorphism, either in the waning stages of contact metamorphism or during regional metamorphism. The nature of the polymetamorphism at Tudor leaves us unable at this time to distinguish between these possibilities. For simplicity of discussion, we will refer to these as products of regional metamorphism. The timing of their formation does not affect the calculation of fluid quantities in the following section.

Reactions 8 and 9 were not encountered in the idealized, plagioclase-free marble compositions we have been considering, so we have not included them in our models. It is worthwhile to consider these reactions further and incorporate them into a comprehensive understanding of the reaction history at Tudor.

The clinozoisite-forming reaction (reaction 9) cannot be modeled reliably at Tudor by eq (3). Reaction 9 differs from the other reactions in that $\partial X(CO_2)/\partial T$ is negative over the $X(CO_2)$ of interest, and, therefore, following the arguments given earlier, eq (3) requires flow to have been down-temperature if it was nearly horizontal. For reaction 8, on the other hand, as with reactions 3 to 7, eq (3) requires up-temperature flow. Because reactions 8 and 9 both appear to be products of regional metamorphism and each requires flow in opposite directions by eq (3), it seems unlikely that simple horizontal flow by this model can apply at Tudor.

Upward vertical fluid flow can also be ruled out as the driving force for reactions 8 and 9. Because dT/dP equals (dT/dz)/(dP/dz), eq (3) becomes

$$q_m = \frac{\nu_i\xi - X_i \sum_j (\nu_j\xi)}{[(\partial X_i/\partial T)_P + (\partial X_i/\partial P)_T(dP/dT)](dT/dz)} \qquad (4)$$

which allows an assessment of metamorphic geothermal gradients. As adjusted for solid solutions, $(\partial X(CO_2)/\partial T)_{4kb} = -5.964264e^{(-0.00481406T)}$ for reaction 9 and $6.987474(10^{-9})e^{(0.0200315T)}$ for reaction 8, and $(\partial X(CO_2)/\partial P)_{500°C} = 5.19003(10^{-7})e^{(0.0007134436P)}$ for reaction 9 and $-2338.3831P^{-2.5050911}$ for reaction 8. Note that these terms have opposite signs for these reactions. Because dT/dz must be negative for upward flow, assuming any normal geothermal gradient, $[\partial X(CO_2)_P/\partial T + (\partial X(CO_2)/\partial P)_T(dP/dT)]$ must be negative for ξ to be positive, regardless of the value of dT/dz. This term can only be negative for reaction 9 at 485°C and 4 kb if $dP/dT < 6.67$ bars/°C and can only be negative for reaction 8 if $dP/dT > 52.3$ bars/°C, and thus there is no

single dP/dT consistent with progress on both of these reactions using the assumptions inherent in eq (4).

Taken together, the best interpretation of these results is that H_2O-rich fluids infiltrated upward and/or outward in the vicinity of the gabbro during regional metamorphism (or late-stages of contact metamorphism). This produced compositional discontinuities across reaction fronts as in the model described earlier for flow of H_2O-rich fluid outward from the pluton. The amounts of reaction were not uniform across the area; some marble contains only reactants of reaction 9, some only product, and others contain both reactants and product (fig. 3G). Therefore, fluid fluxes were variable, and flow was channelized in character.

Because clinozoisite is a product of regional metamorphism, isograd 4 (clinozoisite + amphibole) cannot result from a single event. The H_2O-rich conditions required to stabilize clinozoisite were only realized during regional metamorphism, yet isograd 4 parallels the other isograds whose positions are accounted for by contact metamorphic processes. This paradox is resolved by the polymetamorphism itself. During contact metamorphism, the reactants were unstable according to the reaction

chlorite + 3calcite + 7quartz = anorthite + tremolite + $3CO_2$ + $3H_2O$.

Subsequent regional metamorphism converted plagioclase to clinozoisite by reaction 9. In this way, the mapped isograd (4) is in part the result of contact metamorphism (Chl + Cal + Qtz out) and in part regional metamorphism (Czo in).

Summary of Reaction History

Metamorphism at Tudor must involve at least a two-stage process, early contact metamorphism accompanied by up-temperature fluid flow and later regional metamorphism with channelized infiltration of some marble by H_2O-rich fluid. Contact metamorphism resulted in the formation of mineral reaction isograds 3, 5, 6, and 7 concentric to the pluton. Isograd 3 most likely formed in response to up-temperature fluid flow in the outer aureole. Isograds 5, 6, and 7 formed under T-X(CO_2) conditions near their isobaric thermal maxima and, therefore, were produced largely by thermal processes, although small up-temperature fluid fluxes are possible. Reactions 8 and 9 proceeded either in the waning stages of contact metamorphism or during regional metamorphism in response to local, channelized infiltration of H_2O-rich fluids near the contact.

FLUID QUANTITIES AND COMPARISON OF REGIONAL METAMORPHIC AND POLYMETAMORPHIC MODELS

In the foregoing section, evidence is reviewed that supports the need for a polymetamorphic model to account for the observations in marble near the Tudor gabbro. The purpose of this section is, first, to further quantify the amount of fluid involved in this process and, second, to

compare these results with an alternative "regional metamorphic model" also capable of producing the observed mineral reaction zones. Although the regional metamorphic model ignores the contact metamorphism that had to have occurred, the comparison is useful in illustrating just how model-sensitive fluid flow interpretations are. This comparison is especially justified in this case where all available data are consistent with mineral equilibration during the lower temperature regional metamorphic event. It appears that only carbon isotope exchange in graphite is sufficiently slow that the high-temperature compositions can be preserved.

Fluid/Rock Ratios and Fluid Fluxes

For mineral reactions that are driven by fluid infiltration, a fluid/rock ratio can be determined from the extent of reaction (reaction progress), the composition of the infiltrating fluid, and the equilibrium composition of the pore fluid during reaction. Because the composition of the infiltrating fluid is generally poorly constrained, conventional "water"/rock ratios are calculated assuming pure water as the infiltrant. The result is a minimum fluid/rock ratio (Rice and Ferry, 1982). The "true" fluid/rock ratio can be determined only if the actual infiltrant composition is known and non-reactive fluid flow can be ruled out. Improved "fluid"/rock ratios can be calculated if appropriate infiltrating fluid compositions are applied. Even though the use of fluid/rock ratios has been criticized recently (Baumgartner and Rumble, 1988; Blattner and Lassey, 1990; Baumgartner and Ferry, 1991; Ferry, 1991; Ferry and Dipple, 1991; Bowman, Willett, and Cook, 1994), they are independent of the flow path and can provide a useful measure of the quantity of *externally-derived, reactive* fluid that interacted with a rock during mineral reaction.

Fluid/rock ratios are based on a dimensionless model. The quantity of fluid that has interacted with a rock can also be modeled by one-dimensional flow in which case a flux (for example cm^3/cm^2 or moles/cm^2) is estimated. Fluid flux models may call upon continuous reaction along portions of the flow path or reaction fronts that move in the direction of flow and across which a compositional discontinuity occurs (Hofmann, 1972; Lichtner, 1985; Bickle and McKenzie, 1987; Baumgartner and Rumble, 1988; Baumgartner and Ferry, 1991; Bowman, Willett, and Cook, 1994). Fluid fluxes are sometimes preferable to dimensionless fluid/rock ratios because they monitor all fluid movements rather than only reactive fluids, they include information on flow direction, and they can be coupled to other geochemical or hydrological flow models. However calculation of a fluid flux for real rocks requires greater knowledge of the fluid flow path and reaction kinetics than can generally be assumed. The results of both types of calculations, zero- and one-dimensional, are highly model-dependent and are sensitive to the reaction temperature, especially for reactions with large $dX(CO_2)/dT$ (Wood and Graham, 1986; Baumgartner and Ferry, 1991).

TABLE 6

Inferred reaction temperatures, fluid composition after reaction, and infiltrating fluid compositions used for regional metamorphic and polymetamorphic fluid quantity calculations

	Regional Metamorphic Model			Polymetamorphic Model		
Reaction	T(°C)	reaction $X(CO_2)$	infiltr. $X(CO_2)$	T(°C)	reaction $X(CO_2)$	infiltr. $X(CO_2)$
1	485	0.68	0.29	450	0.40	n.a.
3	485	0.29	0.025	535	0.75	n.a.
				(500)*	(0.44)	n.a.
5	485	0.025	0.010	627	0.75	n.a.
		(0.014)	(0.0040)	(535)	(0.020)	n.a.
6	485	0.010	0.0060	662	0.75	n.a.
7	485	0.0045	0.0040	698	0.75	n.a.
8	485	0.0060	0.0040	485	0.0060	0.0040
9	485	0.010	0.0040	485	0.010	0.0040
		(0.014)	(0.0040)			

n.a., not applicable.
* Values in parentheses apply only to sample 110.

Fluid Quantity Calculations

Fluid/rock ratios and fluid fluxes have been calculated for marble samples at Tudor assuming two different metamorphic histories (summarized in table 6). The first is a regional metamorphic model wherein all reactions took place at 485°C in response to H_2O-rich fluid flow outward from the pluton contact (for example, "Regional Metamorphism" in fig. 10). The second is a polymetamorphic model consistent with up-temperature flow assuming the temperature gradient in figure 4 for reactions 3, 5, 6, and 7 but allows reactions 8 and 9 to take place during regional metamorphism at 485°C (that is a combination of the path in fig. 12 followed by the "Regional Metamorphism" path in fig. 10).

For the regional metamorphic model, fluid/rock ratios are calculated assuming that the composition of the infiltrating fluid is that of the fluid leaving the next up-grade reaction (table 6). A fluid of $X(CO_2) = 0.004$ is assumed to infiltrate at the highest grade to drive reactions 7, 8, and 9 (this is the lowest $X(CO_2)$ allowed at 485°C without wollastonite forming). The number of moles of fluid, Q, with composition $X(CO_2, \text{infl})$, that must have infiltrated in order to drive reaction i to completion is determined from the relationship

$$X(CO_2,\text{rxn}) = \frac{\xi_i n(CO_2)_i + Q\,X(CO_2,\text{infl})}{\xi_i[\nu(CO_2)_i + \nu(H_2O)_i] + Q} \qquad (5)$$

where $X(CO_2,\text{rxn})$ is the pore fluid composition at the point of reaction, ν is the stoichiometric coefficient of fluid species, and ξ_i is the reaction progress that will exhaust some limiting reactant. Reaction progress values are determined from sample modes (table 7) by reconstructing the

entire reaction history of each sample. Fluid/rock ratios thus determined for every reaction that took place in each sample are summed to give the total quantity of fluid required by the model. Reaction 2 is ignored because it involves negligible quantities of fluid. Reaction 1 is included even though there is no "isograd" for this reaction; regional metamorphic grade is everywhere above phlogopite + calcite.

These fluid/rock ratios can be converted to minimum fluid fluxes if multiplied by an appropriate pathlength. This assumes that a flow path can be deduced, that each comparable volume along the path experienced the same flux, and that there is no dispersion in or out of the path. This model presumes that H_2O-rich fluid flowing outward from the contact "pushed" several reaction fronts to their current locations. Thus, a flow pathlength of at least 3000 m is needed to account for the isograd positions, and this is the pathlength used to determine these model fluxes (table 7). These are minimum fluxes because this model does not account for any non-reactive fluids that may have been flushed out ahead of the observed reaction fronts, and the position of reaction 1 is greater than 3000 m. This method yields only crude approximations, but this is adequate for the comparative purposes intended in this study.

The polymetamorphic model employs eq (3) to calculate contact metamorphic fluid fluxes for reactions 1, 3, 5, 6, and 7. A comparison of isograd field locations with the known contact metamorphic thermal gradient (fig. 4) and T-$X(CO_2)$ relations (fig. 6) indicates that reactions 3, 5, 6, and 7 occurred at $X(CO_2)$ values close to 0.75. Reaction 1 is unconstrained and a reaction temperature of 450°C at $X(CO_2) = 0.40$ is assumed for these calculations. Fluid fluxes for reactions 5, 6, and 7 are small at this composition, approaching zero. Only reactions 1 and 3 require any significant fluid flow under these circumstances (table 7). Fluid fluxes determined for each reaction are simply summed to acquire a total flux. This may overestimate the flux needed because the same through-going fluid can, indeed should, participate in all the reactions in its path. However, that assumes the fluid paths are unchanging over the entire reaction history, an unrealistic assumption given the complex dynamics of either contact or regional metamorphism (for example, Hanson, 1992, 1995). Fluid fluxes for the second stage of this model, regional metamorphism, are determined by the same method as the regional metamorphic model.

Sample 110 was treated slightly differently from the rest because it is associated with non-carbonate silicic rocks (fig. 2), and the phase relations for this sample (figs. 6 and 7) suggest that reaction 5 in this area proceeded at a lower temperature, perhaps driven by infiltration. Thus, for this sample, the regional metamorphic model allows reactions 5 and 9 to proceed at $X(CO_2) = 0.014$ (consistent with the currently observed phase equilibria). Because the peak temperature attained by this sample is ~535°C and it lies on the tremolite + K-feldspar isograd, the polymeta-

morphic model for this sample assumes that contact metamorphism drove reaction 3 at 500°C, $X(CO_2) = 0.44$ and reaction 5 (curve labelled $K_5 = 2.98$ in fig. 6) at 535°C, $X(CO_2) = 0.20$. Reaction 9 is treated the same as in the other samples.

TABLE 7

Mineral modes and modeled fluid-reaction histories for selected samples. Mineral abbreviations are given in table 1

Sample	Cal	Qtz	Kfs	Pl	Bi	Am	Czo	Cpx	Grt	Ttn	Other
110	28	5	12	18	3	26	6	—	—	2	trace Py
98	47	3	5	21	8	13	—	—	—	1	1 Gr, 1 (Py, Po, Ilm)
148	38	10	12	10	—	22	4	—	—	2	1 Gr, < 1 Po
63	73	—	—	8	3	4	2	8	—	—	1 Gr, 1 Chl
175	4	2	—	42	—	—	10	35	4	1	2 Py, trace Po

Sample	ctc(m)* (Tmax°C)	Reaction Progress**	Regional Metamorphic Model*** F/R	Regional Metamorphic Model*** Flux	Polymetamorphic Model*** T(°C)	Polymetamorphic Model*** $X(CO_2)$	Polymetamorphic Model*** Flux
110	1300m (535°)	(R1) 18% Bi	0.0051	1,520	~450°	0.40	252
		(R3) 8% Am	0.0058	1,750	~500°	0.44	111
		(R5) 12% Kfs + 18% Am	0.3236	97,080	~535°	0.020	167
		(R9) 6% Czo	0.0220	6,600	~435°	0.014	6,600
			0.3565	106,950			7,130
98	575m (636°)	(R1) 15% Bi	0.0042	1,260	~450°	0.40	192
		(R3) 5% Am	0.0036	1,090	~535°	0.75	49
		(R5) 5% Kfs + 8% Am	0.0378	11,300	~635°	0.75	< 1
			0.0456	13,650			242
148	200m (695°)	(R1) 16% Bi	0.0045	1,350	~450°	0.40	213
		(R3) 4% Am	0.0029	870	~535°	0.75	40
		(R5) 12% Kfs + 18% Am	0.0851	25,510	~635°	0.75	< 1
		(R9) 4% Czo	0.0245	7,340	~485°	0.015	7,340
			0.1170	35,070			7,594
63	37m (724°)	(R1) 3% Bi	0.0008	250	~450°	0.40	39
		(R3) 2% Am	0.0015	440	~535°	0.75	20
		(R5) 1% Kfs + 2% Am	0.0095	2,830	~635°	0.75	< 1
		(R7) 8% Gpx + 2% Bi	1.6250	488,000	~705°	0.75	< 1
		(R9) 2% Czo	0.0122	3,670	~485°	0.015	3,670
			1.6490	495,190			3,731
175	14m (728°)	(R3) 29% Am	0.0211	6,330	~535°	0.75	286
		(R6) 35% Cpx	0.7837	235,000	~660°	0.75	< 1
		(R9) 13% Czo	0.0796	23,900	~485°	0.015	23,900
		(R8) 4% Grt	0.2640	79,200	~485°	0.010	79,200
			1.1484	344,430			103,387

* Distance to the gabbro contact (m) and maximum contact metamorphic temperature in parentheses.

** Reaction progress (reaction in parentheses) forming given quantity of product.

*** Fluid/rock ratios, (moles fluid)/(cm^3 rock), and fluid flux, (moles fluid/cm^2). Temperature and fluid composition of reaction given for the polymetamorphic model. See text for methods.

Comparison of The Regional Metamorphic and Polymetamorphic Models

The results of these models, summarized in table 7, show that less fluid is required for the polymetamorphic scenario. This is especially true for the contact metamorphism. Almost all the fluid required in the polymetamorphic model is for the regional metamorphic reactions (reactions 8 and 9), and these are generous estimates because they assume the same 3000 m pathlength as the regional metamorphic model. In the polymetamorphic scenario, the localized and channelized character of these reactions could be modeled with much smaller fluxes and shorter pathlengths which would increase the difference in fluid quantities required by the two models.

Not only does the regional metamorphic model require more fluid, but, perhaps even more significantly, it requires a fundamentally different manner of fluid flow. In the polymetamorphic model, some rocks may have interacted with relatively small amounts of externally-derived fluid throughout their entire reaction history (for example, sample 98), but the regional metamorphic model requires infiltration of *all* rocks by significant quantities of fluid. Whereas the polymetamorphic model suggests limited, channelized regional metamorphic fluid flow, the regional metamorphic model indicates pervasive flow outward from the gabbro at least as far as the concentric isograds (3 km).

In the Tudor aureole, we see the obvious relationship between the isograds and the pluton; however the calcite-graphite carbon isotope thermometer is the only direct evidence for the size and thermal character of the contact metamorphic aureole (fig. 4). The actual metamorphic process had to be similar to the polymetamorphic model, that is, two steps in T-t-X space, the first similar to the path in figure 12, and the second similar to the "Regional Metamorphic" path in figure 10. Polymetamorphism may be difficult to recognize in many terranes. At Tudor, failure to recognize the polymetamorphism of these rocks would lead to erroneously high estimates of fluid/rock ratios and fluid fluxes and inappropriate interpretations regarding pervasive versus channelized flow.

FLUID INFILTRATION OF THE TUDOR GABBRO

The Tudor gabbro shows widespread evidence for post-crystallization interaction with C–O–H fluids. There were no carbon-bearing phases and few, if any, hydrous phases in the primary igneous mineralogy of the gabbro; some gabbro includes minor hornblende and/or biotite. Much of the gabbro has been recrystallized to hydrous assemblages of actinolitic amphibole, epidote, and albite, ±calcite, ±chlorite, ±oligoclase. Sometimes this metagabbro is weakly foliated, but granoblastic textures are most common, often retaining the original igneous hypidiomorphic-granular texture. The fluid responsible for hydrating and carbonating the gabbro may have been internally-derived late magmatic fluid (deuteric) in part, but there is a tendency for the extent of

hydration and the amount of calcite present to increase near intrusive contacts, suggesting that some or all the fluid was of external origin.

The assemblage epidote + oligoclase + calcite within metagabbro permits quantitative assessment of equilibrium fluid compositions through reaction 9. Results of these calculations for appropriate mineral compositions (table 3) indicate H_2O-rich conditions within the gabbro, $X(CO_2)$ = 0.005 to 0.014 at 485°C, similar to those inferred for marble near the contact (table 4; fig. 7). These fluid compositions represent maximum values of $X(CO_2)$ for the gabbro overall because most metagabbro samples contain only albite rather than oligoclase, and, therefore, lower $X(CO_2)$ is possible. Very low $X(CO_2)$ is also indicated by an occurrence of wollastonite within a marble xenolith (Allen, 1976), which requires $X(CO_2) <$ 0.004 during regional metamorphism.

The quantity of fluid that has infiltrated metagabbro samples can be evaluated from CO_2-flux considerations if we assume that all the CO_2 present in calcite within the gabbro is externally-derived. The maximum solubility of CO_2 in a mafic magma is about 0.25 wt percent at 4 kb (Pan, Holloway, and Hervig, 1991) which could produce 0.65 volume percent calcite at most. However, the correlation of calcite content with proximity to the contact and a significant elevation of $\delta^{18}O$ in metagabbro samples (Dunn, ms; Dunn and Valley, 1996) suggests that a CO_2-bearing, H_2O-rich fluid infiltrated the gabbro and is responsible for providing the CO_2 now forming calcite within metagabbro. If all CO_2 were externally derived, we can estimate minimum quantities of infiltrated fluid.

The calcite-forming reactions also produced albite, epidote, and oxides at the expense of clinopyroxene and labradorite. Regardless of reaction path, each mole of calcite produced required the introduction of at least one mole of CO_2. If the $X(CO_2)$ of the infiltrating fluid is known, then a minimum quantity of externally-derived fluid can be calculated assuming that all infiltrating CO_2 is converted to calcite. The relation between infiltrating fluid composition, modal percentage of calcite formed, and minimum fluid/rock ratios are shown in figure 14. Most metagabbro samples contain between 1 and 4 percent calcite by weight; the average in 42 samples is 2.2 percent calcite, σ = 1.7 (Dunn, ms). For an infiltrating fluid of $X(CO_2)$ = 0.010 (the range of values observed in metagabbro is 0.005-0.014), the minimum fluid/rock ratio required is 0.027 to 0.108 (moles/cm^3). These fluid/rock ratios are similar to those of clinozoisite-bearing marble near the contact, and if a flow path of 1 km is assumed, then fluid fluxes are $\sim 10^4$ moles/cm^2.

DISCUSSION

The polymetamorphic history of marble near the Tudor gabbro illustrates the importance of correctly modeling T–t–X relations in the assessment of fluid-rock interactions in metamorphic rocks. All phase equilibria at Tudor are consistent with the regional metamorphic conditions of ~485°C, 4 kb. Only the calcite-graphite carbon isotope fractionations record the earlier high temperatures. If all reactions are assumed

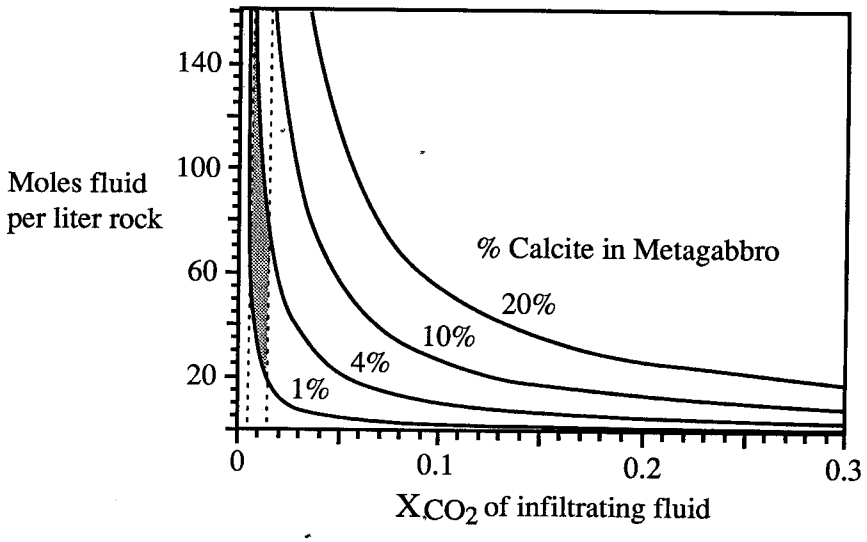

Fig. 14. Minimum amounts of fluid required to introduce sufficient CO_2 to precipitate calcite (1-4 percent) in metagabbro, assuming all the CO_2 is consumed. Infiltrating fluid compositions are constrained by the range of $X(CO_2)$ observed in metagabbro samples, 0.005 to 0.014 (dashed lines). This requires minimum fluid/rock ratios of 0.020 to 0.160 to produce the 1 to 4 percent calcite typical of metagabbro samples.

to occur during regional metamorphism at 485°C, then modeling leads to the erroneous conclusion that a large quantity of fluid pervasively infiltrated marble throughout the area of the concentric isograds, up to 3 km from the contact. Consideration of the polymetamorphic history, however, suggests that the fluid-evolving reactions were largely thermally-driven during contact metamorphism with little or no infiltration except in the outer aureole. This contact event was then overprinted by regional metamorphism and channelized infiltration of H_2O-rich fluids upward along the contact and out into both the pluton and the country-rocks. The results of the polymetamorphic model suggest less pervasive flow and substantially smaller fluid fluxes than the regional metamorphic model.

Modeling of fluid flow within contact aureoles indicates that fluid convection is expected for appropriate thermal gradients and rock permeabilities (Norton and Knight, 1977). The effects of fluid production in the country-rock during contact metamorphism have been incorporated into the models of Hanson (1992, 1995) which show that fluid flow directions can be expected to change over the lifetime of a contact metamorphic event. Much of the fluid production takes place relatively early in the metamorphic event causing an outward flow of the reaction-produced fluid. This stage is followed by development of convective, inward flowing fluids. At Tudor, the development of isograds 5, 6, and 7

may relate to the early expulsion of fluids and isograd 3 to the later convective stage. However, fluid fluxes at Tudor were apparently rather low, even during the convective stage, compared with shallower hydrothermal systems. Convection depends on permeabilities and other factors; the absence of large fluxes at Tudor indicates either low permeability, a low thermal gradient, or a shortage of fluid.

The H_2O-rich fluid flow during regional metamorphism at Tudor was largely confined to within ~1 km of the contact. The reactions driven by infiltration of this fluid are inconsistent with continuous reaction flow models for either up-temperature or down-pressure flow (Baumgartner and Ferry, 1991; Ferry and Dipple 1991) but instead favor a model of H_2O-rich fluid entering the flow path and "pushing" a reaction front forward. An upward, channelized flow mechanism is favored with large variations in local fluid fluxes contributing to variable amphibolitization of the gabbro and variable production of clinozoisite-bearing assemblages in the marble.

The region around sample 110 is dominated by siliciclastic metasedimentary rocks (fig. 2) and coincides with a local metamorphic high. There is no evidence for increased temperatures in this area such that this high represents a local $X(CO_2)$-low. This may indicate higher permeabilities in these low carbonate lithologies relative to marble, allowing greater fluid fluxes. Alternatively, these lithologies may have been capable of greater internal H_2O production during metamorphism and acted, in part, as a source for H_2O. The latter seems unlikely, however, because these rocks appear to have undergone the same reactions as the marble and these produce CO_2-rich fluids.

Possible sources of H_2O-rich fluid during regional metamorphism may be found locally. Siliceous metasediments similar to the Apsley gneiss (Shaw, 1972) or those at Whetstone Lake (Carmichael, 1970) could serve as a source for H_2O-rich fluid during regional metamorphism. In addition, metavolcanic rocks dominated by hydrous phases (chlorite-, epidote-, biotite-, and amphibole-bearing) are locally abundant at the present erosional level. Amphibolite facies metamorphism of these rocks at depth could also serve as a source of H_2O. Even a small percentage of dehydration in any of these formations would produce adequate quantities of H_2O provided it becomes channeled along the gabbro contacts. This contact and those of other intrusions in the area may have served as conduits for dewatering of the crust beneath this relatively low-grade portion of the Grenville Province.

Comparison of Tudor to Other Areas

Many contact metamorphic aureoles produced at low pressures differ from Tudor in that they contain minerals indicative of very low $X(CO_2)$, including wollastonite, periclase, or vesuvianite; for example, Crestmore, California; Alta, Utah; Notch Peak, Utah; and Christmas Mountains, Texas (Burnham, 1959; Moore and Kerrick, 1976; Labotka, Nabelek, and Papike, 1988; Joesten, 1976). Wollastonite in the high

grade zone of a contact aureole requires either very high temperatures or H_2O-rich conditions at the time of metamorphism. Wollastonite is more likely in shallow contact aureoles because lower pressure stabilizes wollastonite to lower temperature, and access to surface derived water is increased (Valley and O'Neil, 1982). The peak of contact metamorphism at Tudor was not accompanied by H_2O-rich conditions, and this may reflect the depth of intrusion and unavailability of surface waters.

Internal buffering to high $X(CO_2)$ within carbonate rocks during contact metamorphism is described at several localities, the classic example being the Marysville aureole, Montana (Rice, 1977). Other examples include the Elkhorn aureole, Montana (Bowman and Essene, 1982), Notch Peak aureole, Utah (Hover-Granath, Papike, and Labotka, 1983; Nabelek and others, 1984; Labotka, Nabelek, and Papike, 1988), and the Ballachulish aureole, Scotland (Masch and Heuss-Aßbichler, 1991). However, at Alta, Elkhorn, and Ballachulish, peak metamorphic periclase indicates H_2O-rich conditions near these intrusions (Moore and Kerrick, 1976; Bowman and Essene, 1982; Masch and Heuss-Aßbichler, 1991). Thus, except for the innermost portions of contact aureoles, carbonate lithologies commonly buffer fluids to CO_2-rich compositions.

Many carbonate-bearing rocks exhibit H_2O-rich fluid conditions proximal to igneous contacts, and stable isotopic studies suggest that in many of these the H_2O was of magmatic origin (Taylor and O'Neil, 1977; Nabelek and others, 1984; Nabelek, Labotka, and Russ-Nabelek, 1992; Bowman, O'Neil, and Essene, 1985; Bowman, Willett, and Cook, 1994; Brown, Bowman, and Kelly, 1985; Jamtveit, Bucher-Nurminen, and Stijfhoorn, 1992). Stable isotopic data from Tudor, however, does not support a magmatic source for the H_2O infiltration of Tudor marbles (Dunn, ms; Dunn and Valley, 1996), and this may reflect the lower water content of mafic plutons such as the Tudor. Other contact aureoles also show evidence of late hydration, such as the conversion of periclase to brucite after peak temperatures subsided, but in these cases, unlike Tudor, H_2O-rich conditions are indicated for peak temperatures as well (Moore and Kerrick, 1976; Bowman and Essene, 1982).

Many regional metamorphic terranes as well as contact aureoles exhibit "the H_2O problem", that is, fluids become H_2O-rich at high grades, although CO_2-rich fluids are produced by the prograde reactions. This observation has been interpreted to require a large, pervasive influx of H_2O to drive the reactions by diluting the fluid produced (Ferry, 1984, 1986, 1992). At Tudor, the H_2O influx clearly postdates the peak metamorphic conditions which leads to a very different interpretation, namely lesser quantities of fluid and a channelized mode of infiltration.

Is All Metamorphism "Polymetamorphic"?

The temporal distinction of more than one fluid-rock interaction event at Tudor is not unique. Even a single metamorphic episode can be "polymetamorphic" if fluid conditions change dramatically over the lifetime of the event. Many, if not most, metamorphic terranes are

characterized by more than a single thermal pulse or by the introduction of retrograde fluids after peak temperatures are attained. Even in the relatively simple example of a contact aureole, fluid flow conditions are *expected* to change over the course of time (Dutrow, 1990; Manning and Bird, 1991; Hanson, 1992, 1995). A separation in timing of fluid conditions during metamorphism might be an important factor for interpreting other areas of the Grenville, for example along the northern margin of the Thanet Gabbro (LeAnderson and Munoz, 1987) and in the Whetstone Lake area (Carmichael, 1970), as well as in other metamorphic terranes.

Metamorphic terranes evolve along P–T–t paths such that even in a "single-metamorphic" episode, rocks undergo sequential mineral reactions in response to the changing pressure-temperature-fluid conditions. Impure carbonate systems are particularly predisposed to changing fluid conditions as reactions that evolve different compositions of fluid are encountered at various points along the P–T–t path. The final equilibrium state imposed on the system will generally be an imperfect model for earlier states and in most cases, including Tudor, models based solely on the final state will lead to grossly incorrect conclusions, in particular, erroneously large fluid fluxes.

Given the complex nature of metamorphic episodes, with continuously changing temperatures and pressures, shifting thermal and baric gradients, and variations in the timing and location of mineral reactions, it is reasonable to postulate that fluid conditions will also change substantially over the course of metamorphism. Models that do not account for P–T–t–X variation may produce incomplete or inaccurate results.

ACKNOWLEDGMENTS

This work was supported by the American Chemical Society Petroleum Research Fund (18839-AC2), the National Science Foundation (EAR 8805470 to JV, EAR 9305104 to SD), the Gas Research Institute (5086-260-1425), the Geological Society of America (Penrose grant 3416-85). SRD also gratefully acknowledges the UW Alumni Research Fund, the Shell Foundation, and the Louis G. Weeks Fund, University of Wisconsin-Madison. We thank Everett Glover for guidance in the microprobe laboratory at the UW Department of Geology and Geophysics, and we appreciate the encouragement of Dugald Carmichael. We thank P.E. Brown, M.L. Crawford, W.A. Crawford, J.J. Ague, and M.L. Gerdes for comments on an earlier version of the manuscript. We are grateful for reviews by Greg Dipple and an anonymous reviewer. Greg Dipple's comments proved particularly helpful. Thanks also to Danny Rye for his patience.

APPENDIX I

Equilibria methods and constraints

All equilibria were calculated using the thermodynamic data of Berman (1988) and the equation of state for H_2O-CO_2 mixtures of Kerrick and Jacobs (1981). Equilibrium con-

TABLE 8

Activity formulas utilized for equilibrium calculations. Mineral abbreviations as in table 1

$\alpha_{An} = X(Ca)\gamma_{An}$ (1)	$\alpha_{Kfs} = X(K)$
$\alpha_{Grs} = X(Ca)^3X(Al)^2$ (2)	$\alpha_{Di} = X(Ca)X(Mg)$
$\alpha_{Phl} = X(K)X(Mg)^3X(OH)^2$	$\alpha_{Cal} = X(Ca)$
$\alpha_{Czo} = \alpha_{Zo} = X(Ca)\ ^2X(Al, M3)X(OH)$ (3)	
$\alpha_{Tr} = X(Ca)^2X(Mg, M1, 3)^5X(Mg, M2)^2X(Si, T1)^4X(OH)^2$ (4)	

(1) $\gamma_{An} \cong 1.85$, see app. 1.
(2) $\alpha_{Grs} \cong X(Ca)^3X(Al)^2$ at $X_{Grs} > 0.9$ (Engi and Wersin, 1987).
(3) Fe^{3+} partitioned into M3 (Dollase, 1973). Clinozoisite-pistacite solutions are nearly ideal for < 0.2 pistacite, $Ca_2Fe_3Si_3O_{12}(OH)$ (Bird and Helgeson, 1980).
(4) Site assignment and formula from Blundy and Holland (1990).

stants were calculated for constraining equilibria (table 1) using mineral compositions in table 3 and the activity formulations summarized in table 8. Results are reported in table 4.

Application of reaction 9 requires estimation of anorthite activities at rather dilute solutions. The activity-composition relations for this system are poorly known at 500°C and relations are likely to be non-ideal, especially near the peristerite solvus. Anorthite activities calculated by the Al-avoidance method of Newton, Charlu, and Kleppa (1980) are similar to estimates determined by other methods for sodic compositions at temperatures ~500°C (see comparisons by Carpenter and Ferry, 1984). Thus, activity coefficients of ~1.85, consistent with Newton, Charlu, and Kleppa (1980) and also with the order/disorder model of Carpenter and Ferry (1984) have been applied.

The composition of metamorphic fluids in marble distal to the Tudor gabbro can be constrained by reaction 1. Allen (1976) reports chemical analyses of six biotites coexisting with dolomite, calcite, and quartz from samples on the low-grade side of isograd 3. These samples contain no K-feldspar ($\alpha_{Kfs} \leq 1$), and minimum values of K_1 can be calculated for the limiting case where $\alpha_{Kfs} = 1.0$. These values of K_1 are ≤ 0.170 which indicate that $X(CO_2) \leq 0.69$ at 485°C (fig. 6). Allen also gives analyses of amphibole, calcite, and dolomite in five isobarically univariant quartz-bearing samples from isograd 3 north of the Tudor gabbro which yield $K_3 = 0.291$ to 0.509. Thus, at the metamorphic temperature of 485°C, marble at isograd 3 has $X(CO_2) = 0.25$ to 0.28 (fig. 6).

Sample 98 contains biotite + calcite + quartz + amphibole + K-feldspar + plagioclase and, therefore, is on isograd 5 and on the CO_2-rich side of reaction 9. K_5 for this sample equals 64.1 which yields $X(CO_2) = 0.025$ at 485°C (fig. 7). Independent of temperature, this assemblage permits an estimate of the minimum $X(CO_2)$. The sample contains no clinozoisite, but a reasonable estimate for the minimum value of K_9 can be obtained by comparison with sample 148. Sample 148 contains amphibole and plagioclase compositionally similar to those in sample 98 (table 3) and the value of K_9 for sample 148 is 4.29. Thus, sample 98 requires higher $X(CO_2)$ than the intersection of reaction 5 ($K_5 = 64.1$) and reaction 9 ($K_9 = 4.29$), that is $X(CO_2) \geq 0.014$. This is consistent with $X(CO_2) = 0.025$ from assuming T = 485°C.

Sample 110 contains biotite + calcite + quartz + amphibole + K-feldspar + plagioclase + clinozoisite and, therefore, lies at the intersection of reaction 5 ($K_5 = 2.98$) and reaction 9 ($K_9 = 5.57$). At 4 kb, this invariant point indicates a temperature of 435°C and $X(CO_2)$ of 0.014 (fig. 7). This temperature is close to the inferred peak of regional metamorphism at 485°C.

Sample 148 contains amphibole + calcite + quartz + K-feldspar + plagioclase + clinozoisite and, therefore, lies above isograd 5, below reaction 14, and on reaction 9

($K_9 = 4.29$). Thus, this sample requires temperatures below ~525°C and $X(CO_2) \geq 0.010$. At 485°C, $X(CO_2)$ equals 0.012.

Sample 63 contains amphibole + calcite + clinopyroxene + biotite + clinozoisite + albite and, therefore, lies above isograd 7 and on the low CO_2 side of reaction 9. Because calcite + quartz assemblages occur throughout this area and wollastonite is absent, we can infer that this sample also lies below reaction 14. This sample contains no K-feldspar ($\alpha_{Kfs} \leq 1$) and, therefore, $K_7 \geq 1{,}790$. In the absence of oligoclase, the maximum K_9 possible for this sample can be obtained by assuming an anorthite activity for An20, the anorthite-rich side of the peristerite solvus. This yields $K_9 \geq 16.6$ and in the absence of wollastonite ($K_{14} \leq 1$) constrains this sample to the stippled area in figure 7, $X(CO_2) \leq 0.0045$ and $T \leq 485$°C.

Sample 175 contains the assemblage garnet + clinozoisite + calcite + quartz + albite and, therefore, lies on reaction 8 and on the low temperature side of the intersection of reaction 8 with reactions 16 and 9. The position of equilibria $K_8 = 4.17$ is shown in figure 7 (curve labelled 8'). In the absence of oligoclase, the maximum K_9 possible for this sample can be obtained by assuming An20, the anorthite-rich side of the peristerite solvus. This yields $K_9 \geq 3.75$ and $K_{16} \leq 0.178$ and requires $X(CO_2) \leq 0.012$ and $T \leq 520$°C (fig. 7).

References

Allen, J. M., ms 1976, Silicate-carbonate equilibria in calcareous metasediments of the Tudor Township area, Ontario: a test of the P-T-$X(CO_2)$-$X(H_2O)$ model of metamorphism: Ph.D. thesis, Queens University, Kingston, Ontario, Canada, 227 p.

Anovitz, L. M., and Essene, E. J., 1987, Phase equilibria in the system $CaCO_3$-$MgCO_3$-$FeCO_3$: Journal of Petrology, v. 28, p. 389–414.

———— 1989, Thermobarometry and pressure-temperature paths in the Grenville Province of Ontario: Journal of Petrology, v. 31, p. 197–241.

Baker, J., Bickle, M. J., Buick, I. S., Holland, T. J. B., and Mathews, A., 1989, Isotopic and petrologic evidence for the infiltration of water-rich fluids during the Miocene M2 metamorphism on Naxos, Greece: Geochimica et Cosmochimica Acta, v. 53, p. 2037–2050.

Baksi, A. K., 1982, 40Ar-39Ar incremental heating studies on the Tudor gabbro, Grenville Province, Ontario: its bearing on the North American apparent polar wander path in late Proterozoic times: Geophysical Journal of the Astronomical Society, v. 70, p. 545–562.

Baumgartner, L. P., and Ferry, J. M., 1991, A model for coupled fluid flow and mixed volatile mineral reactions with applications to regional metamorphism: Contributions to Mineralogy and Petrology, v. 106, p. 273–285.

Baumgartner, L. P., and Rumble, D. III, 1988, Transport of stable isotopes: I. Development of a continuum theory for stable isotope transport: Contributions to Mineralogy and Petrology, v. 98, p. 417–430.

Bell, K., and Blenkinsop, J., 1980, Whole-rock Rb-Sr studies in the Grenville Province in southeastern Ontario and western Quebec—a summary report, in Current Research, Part C: Geological Survey of Canada, Paper 80-1C, p. 152–153.

Berger, G. W., and York, D., 1981, 40Ar/39Ar dating of the Thanet gabbro, Ontario: looking through the Grenvillian metamorphic veil and implications for paleomagnetism: Canadian Journal of Earth Science, v. 18, p. 266–273.

Berman, R. G., 1988, Internally-consistent thermodynamic data for minerals in the system Na_2O-K_2O-CaO-MgO-FeO-Fe_2O_3-SiO_2-TiO_2-H_2O-CO_2: Journal of Petrology, v. 29, p. 445–522.

Bickle, M. J., and Baker, J., 1990, Advective-diffusive transport of isotopic fronts: an example from Naxos, Greece: Earth and Planetary Science Letters, v. 97, p. 78–93.

Bickle, M. J., and McKenzie, D., 1987, The transport of heat and matter by fluids during metamorphism: Contributions to Mineralogy and Petrology, v. 95, p. 384–392.

Bird, D. K., and Helgeson, H. C., 1980, Chemical interaction of aqueous solutions with epidote-feldspar mineral assemblages in geologic systems. 1. Thermodynamic analysis of phase relations in the system CaO-FeO-Fe_2O_3-SiO_2-H_2O-CO_2: American Journal of Science, v. 280, p. 907–941.

Blattner, P., and Lassey, K. R., 1990, Transport of stable isotopes, kinetics, dispersive advection, and the 'isotopic fronts' of Baumgartner and Rumble (1988): Contributions to Mineralogy and Petrology, v. 105, p. 486–490.

Blundy, J. D., and Holland, T. J. B., 1990, Calcic amphibole equilibria and a new amphibole-plagioclase geothermometer: Contributions to Mineralogy and Petrology, v. 104, p. 208–224.

Bowman, J. R., and Essene, E. J., 1982, P-T-X(CO_2) conditions of contact metamorphism in the Black Butte aureole, Elkhorn, Montana: American Journal of Science, v. 282, p. 311–340.

Bowman, J. R., O'Neil, J. R., and Essene, E. J., 1985, Contact skarn formation at Elkhorn, Montana. II: Origin and evolution of C-O-H skarn fluids: American Journal of Science, v. 285, p. 621–660.

Bowman, J. R., Willett, S. D., and Cook, S. J., 1994, Oxygen isotopic transport and exchange during fluid flow: one-dimensional models and applications: American Journal of Science, v. 294, p. 1–55.

Brown, P. E., Bowman, J. R., and Kelly, W. C., 1985, Petrologic and stable isotope constraints on the source and evolution of skarn-forming fluids at Pine Creek, California: Economic Geology, v. 80, p. 72–95.

Burnham, C. W., 1959, Contact metamorphism of magnesian limestones at Crestmore, California: Geological Society of America Bulletin, v. 70, p. 879–920.

Carmichael, D. M., 1970, Intersecting isograds in the Whetstone Lake area, Ontario: Journal of Petrology, v. 11, p. 147–181.

Carmichael, D. M., Moore, Jr., J. M., and Skippen, G. B., 1978, Isograds around the Hastings metamorphic "low": Geological Association of Canada and Mineralogical Association of Canada, Annual Meeting, Toronto, Field Trips Guidebook, 1978, p. 325–345.

Carpenter, M. A., and Ferry, J. M., 1984, Constraints on the thermodynamic mixing properties of plagioclase feldspars: Contributions to Mineralogy and Petrology, v. 87, p. 138–148.

Cartwright, I., and Valley, J. W., 1991, Steep oxygen-isotope gradients at marble-metagranite contacts in the northwest Adirondack Mountains, New York, USA: products of fluid-hosted diffusion: Earth and Planetary Science Letters, v. 107, p. 148–163.

Corriveau, L., Heaman, L. M., Marcantonio, F., and van Breeman, O., 1990, 1.1 Ga K-rich alkaline plutonism in the SW Grenville Province: Contributions to Mineralogy and Petrology, v. 105, p. 473–485.

Cosca, M. A., Sutter, J. F., and Essene, E. J., 1991, Cooling and inferred uplift/erosion history of the Grenville Orogen, Ontario: constraints from $^{40}Ar/^{39}Ar$ thermochronology: Tectonics v. 10, p. 959–977.

Criss, R. E., and Taylor, Jr., H. P., 1986, Meteoric-hydrothermal systems, *in* Valley, J. W., Taylor, Jr., H. P., and O'Neil, J. R., editors, Stable Isotopes in High Temperature Geological Processes: Mineralogical Society of America, Reviews in Mineralogy, v. 16, p. 373–424.

Davis, D. W., and Bartlett, J. R., 1988, Geochronology of the Belmont metavolcanic complex and implications for crustal development in the Central Metasedimentary Belt, Grenville Province, Ontario: Canadian Journal of Earth Science, v. 25, p. 1751–1759.

Dollase, W. A., 1973, Mossbauer spectra and iron distribution in the epidote-group minerals: Zeitschrift fur Kristallographie, v. 138, p. 41–63.

Dunn, S. R., ms, 1989, Metamorphism and stable isotope geochemistry of the Tudor gabbro and adjacent marble, Ontario, Canada: Ph.D. thesis, University of Wisconsin, Madison, 245 p.

Dunn, S. R., and Valley, J. W., 1992, Calcite-graphite isotope thermometry: a test for polymetamorphism in marble, Tudor gabbro aureole, Ontario: Journal of Metamorphic Geology, v. 10, p. 487–501.

———— 1996, Metamorphic fluid-rock interaction in the Tudor metagabbro and adjacent marble: stable isotope evidence. in preparation.

Dutrow, B., 1990, Pore fluid pressure and the timing of fluid-mineral interaction in contact metamorphic settings: a preliminary analysis: Geological Society of American Abstracts with Programs, v. 22, no. 7, p. A213.

Easton, R. M., 1986, Geochronology of the Grenville Province, *in* Moore, J. M., Davidson, A., and Baer, A. J., editors, The Grenville Province: Geological Association of Canada Special Paper 31, p. 127–173.

Engi, M., and Wersin, P., 1987, Derivation and application of a solution model for calcic garnet: Schweizerische Mineralogische und Petrographische Mitteilungen, v. 67, p. 53–73.

Etheridge, M. A., Wall, V. J., and Vernon, R. H., 1983, The role of the fluid phase during regional metamorphism and deformation: Journal of Metamorphic Geology, v. 1, p. 205–226.
Ferry, J. M., 1984, A biotite isograd in south-central Maine, U.S.A.: mineral reactions, fluid transfer, and heat transfer: Journal of Petrology, v. 25, p. 871–893.
———— 1986, Infiltration of aqueous fluid and high fluid:rock ratios during greenschist facies metamorphism: a reply: Journal of Petrology v. 27, p. 695–714.
———— 1991, Dehydration and decarbonation reactions as a record of fluid infiltration, *in* Kerrick, D. M., editor, Contact Metamorphism: Mineralogical Society of America, Reviews in Mineralogy, v. 26, p. 351–393.
———— 1992, Regional metamorphism of the Waits River Formation, eastern Vermont: delineation of a new type of giant metamorphic hydrothermal system: Journal of Petrology, v. 33, p. 45–94.
Ferry, J. M., and Dipple, G. M., 1991, Fluid flow, mineral reactions, and metasomatism: Geology, v. 19, p. 211–214.
———— 1992, Models for coupled fluid flow, mineral reaction, and isotopic alteration during contact metamorphism: the Notch Peak aureole, Utah: American Mineralogist, v. 77, p. 577–591.
Greenwood, H. J., 1975, Buffering of pore fluids by metamorphic reactions: American Journal of Science, v. 275, p. 573–593.
Hanson, R. B., 1992, Effects of fluid production on fluid flow during regional and contact metamorphism: Journal of Metamorphic Geology, v. 10, p. 87–97.
———— 1995, The hydrodynamics of contact metamorphism: Geological Society of America Bulletin, v. 107, p. 595–611.
Hayatsu, A., and Palmer, H. C., 1975, K-Ar isochron study of the Tudor gabbro, Grenville Province, Ontario: Earth and Planetary Science Letters, v. 25, p. 208–212.
Hewitt, D. F., 1962, Geology of Wollaston Township, Hastings County: Ontario Department of Mines, Toronto, Geological Report 11, p. 29–55.
———— 1968, Geology of Madoc Township and the northern part of Huntington Township, Hastings County: Ontario Department of Mines, Toronto, Geological Report 73, 45 p.
Hofmann, A. W., 1972, Chromatographic theory of infiltration metasomatism and its application to feldspars: American Journal of Science, v. 272, p. 69–90.
Holdaway, M. J., 1971, Stability of andalusite and the aluminum silicate phase diagram: American Journal of Science, v. 271, p. 97–131.
Hover-Granath, V. C., Papike, J. J. and Labotka, T. C., 1983, The Notch Peak contact metamorphic aureole, Utah: petrology of the Big Horse limestone member of the Orr Formation: Geological Society of America Bulletin, v. 94, p. 889–906.
Jacobs, G. K., and Kerrick, D. M., 1981, Devolatilization equilibria in H_2O-CO_2 and H_2O-CO_2-NaCl fluids: an experimental and thermodynamic evaluation at elevated pressures and temperatures: American Mineralogist, v. 66, p. 1135–1153.
Jaeger, J. C., 1959, Temperatures outside a cooling intrusive sheet: American Journal of Science, v. 257, p. 44–54.
———— 1964, Thermal effects of intrusions: Reviews of Geophysics, v. 2, p. 443–466.
Jamtveit, B., Bucher-Nurminen, K., and Stijfhoorn, D. E., 1992, Contact metamorphism of layered shale-carbonate sequences in the Oslo Rift: I. buffering, infiltration, and mechanisms of mass transport: Journal of Petrology, v. 33, p. 377–422.
Joesten, R., 1976, High-temperature contact metamorphism of carbonate rocks in a shallow crustal environment, Christmas mountains, Big Bend region, Texas: American Mineralogist, v. 61, p. 776–781.
Kerrick, D. M., and Jacobs, G. K., 1981, A modified Redlich-Kwong equation for H_2O, CO_2, and H_2O-CO_2 mixtures at elevated pressures and temperatures: American Journal of Science, v. 281, p. 736–767.
Kitchen, N. E., and Valley, J. W., 1995, Carbon isotope thermometry in marbles of the Adirondack Mountains, New York: Journal of Metamorphic Geology, v. 13, p. 577–594.
Laakso, R. K., 1968, Geology of Lake Township, Hastings County: Toronto, Ontario Department of Mines, Geological Report 54, 36 p.
Labotka, T. C., Nabelek, P. I., and Papike, J. J., 1988, Fluid infiltration through the Big Horse limestone member in the Notch Peak contact-metamorphic aureole, Utah: American Mineralogist, v. 73, p. 1302–1324.
Lamb, W. M., ms, 1987, Metamorphic fluids and granulite genesis: Ph.D. thesis. University of Wisconsin, Madison, Wisconsin, USA, 234 p.

Lamb, W. M., and Valley, J. W., 1984, Metamorphism of reduced granulites in low-CO_2 vapour-free environments: Nature, v. 312, p. 56–58.

———— 1985, C-O-H fluid calculations and granulite genesis, *in* Tobi, A. C., and Touret, J. L. R., editors, The Deep Proterozoic Crust in the North Atlantic Provinces: Dordrecht, the Netherlands, D. Reidel Publishing Company, p. 119–131.

Lasaga, A. C., and Rye, D. M., 1993, Fluid flow and chemical reaction kinetics in metamorphic systems: American Journal of Science, v. 293, p. 361–401.

LeAnderson, P. J., and Munoz, J. L., 1987, Relationship between rock type, metamorphic grade, and fluid phase composition in the Grenville Supergroup, Limerick Township, Ontario: Canadian Mineralogist, v. 25, p. 485–498.

Lichtner, P. C., 1985, Continuum model for simultaneous chemical reactions and mass transport in hydrothermal systems: Geochimica et Cosmochimica Acta, v. 49, p. 779–800.

Lumbers, S. B., 1969, Geology of Limerick and Tudor Townships, Hastings County: Ontario Department of Mines, Toronto, Geological Report 67, 110 p.

Lumbers, S. B., Heaman, L. M., Vertolli, V. M., and Wu, T-W., 1990, Nature and timing of Middle Proterozoic magmatism in the Central Metasedimentary Belt, Grenville Province, Ontario, *in* Gower, C. F., Rivers, T., and Ryan, A. B., editors, Mid-Proterozoic Laurentia-Baltica: Geological Association of Canada Special Paper 38, p. 243–276.

Manning, C. E., and Bird, D. K., 1991, Porosity evolution and fluid flow in the basalts of the Skaergaard magma-hydrothermal system, east Greenland: American Journal of Science, v. 291, p. 201–257.

Masch, L., and Heuss-Aßbichler, S., 1991, Decarbonation reactions in siliceous dolomites and impure limestones, *in* Voll, G., Topel, J., Pattison, D. R. M., and Seifert, F., editors, Equilibrium and Kinetics in Contact Metamorphism: the Ballachullish Igneous Complex and its Aureole: Berlin, Springer-Verlag, p. 211–227.

Meyers, J., and Eugster, H. P., 1983, The system Fe-Si-O: oxygen buffer calibrations to 1,500K: Contributions to Mineralogy and Petrology, v. 82, p. 75–90.

Mezger, K., Essene, E. J., van der Pluijm, B. A., and Haliday, A. N., 1993, U-Pb geochronology of the Grenville Orogen of Ontario and New York: constraints on ancient crustal tectonics: Contributions to Mineralogy and Petrology, v. 114, p. 13–26.

Moore, J. N., and Kerrick, D. M., 1976, Equilibria in siliceous dolomites of the Alta aureole, Utah: American Journal of Science, v. 276, p. 502–524.

Nabelek, P. I., Labotka, T. C., O'Neil, J. R., and Papike, J. J., 1984, Contrasting fluid/rock interaction between the Notch Peak granitic intrusion and argillites and limestones in western Utah: evidence from stable isotopes and phase assemblages: Contributions to Mineralogy and Petrology, v. 86, p. 25–34.

Nabelek, P. I., Labotka, T. C., and Russ-Nabelek, C., 1992, Stable isotope evidence for the role of diffusion, infiltration, and local structure on contact metamorphism of calc-silicate rocks at Notch Peak, Utah: Journal of Petrology, v. 33, p. 557–583.

Newton, R. C., Charlu, T. V., and Kleppa, O. J., 1980, Thermochemistry of the high structural state plagioclases: Geochimica et Cosmochimica Acta, v. 44, p. 933–941.

Norton, D., and Knight, J., 1977, Transport phenomena in hydrothermal systems: cooling plutons: American Journal of Science, v. 277, p. 937–981.

Orville, P. M., 1972, Plagioclase cation exchange equilibria with aqueous chloride solution: results at 700°, 2000 bars in the presence of quartz: American Journal of Science, v. 272, p. 234–272.

Pan, V., Holloway, J. R., and Hervig, R. L., 1991, The pressure and temperature dependence of carbon dioxide solubility in tholeiitic basalt melts: Geochimica et Cosmochimica Acta, v. 55, p. 1587–1595.

Rice, J. M., 1977, Progressive metamorphism of impure dolomitic limestone in the Marysville aureole, Montana: American Journal of Science, v. 277, p. 1–24.

Rice, J. M., and Ferry, J. M., 1982, Buffering, infiltration, and the control of intensive variables during metamorphism, *in* Ferry, J. M., editor, Characterization of Metamorphism through Mineral Equilibria: Mineralogical Society of America, Reviews in Mineralogy, v. 10, p. 263–353.

Shaw, D. M., 1962, Geology of Chandos Township, Peterborough County: Ontario Department of Mines, Toronto, Geological Report 11, p. 1–28.

———— 1972, Origin of the Apsley gneiss: Canadian Journal of Earth Sciences, v. 9, p. 18–35.

Shmonov, V. M., and Shmulovich, K. I., 1974, Molal volumes and equation of state of CO_2 at temperatures from 100 to 1000°C and pressures from 2000 to 10,000 bars: Akademii Nauk SSSR Doklady, v. 217, p. 206–209.

Silver, L. T., and Lumbers, S. B., 1966, Geochronological studies in the Bancroft-Madoc area of the Grenville Province, Ontario, Canada: Geological Society of America, Abstracts with Programs, v. 87, p. 156.
Smith, J. V., 1983, Phase equilibria of plagioclase, in Ribbe, P. H., ed., Feldspar Mineralogy: Mineralogical Society of America, Reviews in Mineralogy, v. 2, 2nd ed., p. 223–239.
Sobol, J. W., ms, 1973, The petrology of Grenville marbles in the vicinity of Bancroft, Ontario: M.S. thesis, University of Michigan, 45 p.
Sobol, J. W., and Essene, E. J., 1973, Petrology of Grenville marbles from southern Ontario: Geological Society of America, Abstracts with Programs, v. 5, p. 815.
Taylor, B. E., and O'Neil, J. R., 1977, Stable isotope studies of metasomatic Ca-Fe-Al-Si skarns and associated metamorphic and igneous rocks, Osgood, Mountains, Nevada: Contributions to Mineralogy and Petrology, v. 63, p. 1–49.
Taylor, H. P., Jr., and Forester, R. W., 1979, An oxygen and hydrogen isotope study of the Skaergaard intrusion and its country rocks: a description of a 55 m.y. old fossil hydrothermal system: Journal of Petrology, v. 20, p. 355–419.
Valley, J. W., 1986, Stable isotope geochemistry of metamorphic rocks, *in* Valley, J. W., Taylor, H. P., Jr., and O'Neil, J. R., editors, Stable Isotopes in High Temperature Processes: Mineralogical Society of America, Reviews in Mineralogy, v. 16, p. 445–489.
Valley, J. W., Bohlen, S. R., Essene, E. J., and Lamb, W., 1990, Metamorphism in the Adirondacks: II. The role of fluids: Journal of Petrology, v. 31, p. 555–596.
Valley, J. W., and O'Neil, J. R., 1981, $^{13}C/^{12}C$ exchange between calcite and graphite: a possible thermometer in Grenville marbles: Geochimica et Cosmochimica Acta, v. 45, p. 411–419.
———— 1982, Stable isotope evidence for shallow emplacement of Adirondack anorthosite: Nature, v. 300, p. 497–500.
———— 1984, Fluid heterogeneity during granulite facies metamorphism in the Adirondacks: stable isotope evidence: Contributions to Mineralogy and Petrology, v. 85, p. 158–173.
Wada, H., and Suzuki, K., 1983, Carbon isotope thermometry calibrated by dolomite-calcite solvus temperatures: Geochimica et Cosmochimica Acta, v. 47, p. 697–706.
Walther, J. V., and Orville, P. M., 1982, Volatile production and transport in regional metamorphism: Contributions to Mineralogy and Petrology, v. 79, p. 252–257.
Wood, B. J., and Graham, C. M., 1986, Infiltration of aqueous fluid and high fluid:rock ratios during greenschist facies metamorphism: a discussion: Journal of Petrology, v. 27, p. 751–761.